Ocean Systems Engineering, *Vol. 9, No. 1 (2019) 43-77*
DOI: https:// doi.org/10.12989/ose.2019.9.1.043

A site-specific CFD study of passing ship effects on multiple moored ships

Hamn-Ching Chen[*1], Chia-Rong Chen[1] and Erick T. Huang[2]

[1]*Zachry Department of Civil Engineering, Texas A&M University, College Station, Texas 77843, USA*
[2]*Engineering and Expeditionary Warfare Center, Naval Facilities Engineering Command, Port Hueneme California 93043, USA*

(Received November 3, 2018, Revised January 10, 2019, Accepted January 14, 2019)

Abstract. A local-analytic-based Navier-Stokes solver has been employed in conjunction with a compound ocean structure motion analysis program for time-domain simulation of passing ship effects induced by multiple post-Panamax class ships in the exact condition of a real waterway. The exact seabed bathymetry was reproduced to the utmost precision attainable using the NOAA geophysical database for Virginia Beach, NOAA nautical charts for Hampton Roads and Norfolk harbor, and echo sounding data for the navigation channel and waterfront facilities. A parametric study consists of 112 simulation cases with various combinations of ship lanes, ship speeds, ship heading (inbound or outbound), channel depths, drift angles, and passing ship coupling (in head-on or overtaking encounters) were carried out for two waterfront facilities at NAVSTA Norfolk and Craney Island Fuel Terminal. The present paper provides detailed parametric study results at both locations to investigate the site-specific passing ship effects on the motion responses of ships moored at nearby piers.

Keywords: passing ship effects; site-specific; computational fluid dynamics; moving overset grids; coupled motion analysis

1. Introduction

A federal navigation channel passes to the west of the Naval Station (NAVSTA) Norfolk waterfront and to the east of Craney Island as shown in Fig. 1, with north to the left. The federal authority has launched a plan to reconfigure the channel to mitigate the passing ship effects resulted from the ever-increasing ship sizes after recent Panama Canal expansion. A detailed description of the facility layouts and passing ship scenarios can be found in Huang, Chen and Chen (2018).

Pressure pulses and wakes induced by passing ships are known hazards to moored vessels nearby. Excessive disturbances often interrupt ship operations at the pier or cause damages to ship hulls, pier structures, and interface outfits. Passing ships are normally regulated to cruise in designated lanes within allowable speed limits that do not hamper the efficiency of the waterway or compromise pier operations nearby. Key parameters dictating the passing ship effects include the lateral distance of ship lanes to piers, the size and speed of passing ships, the depth of

*Corresponding author, A.P. & Florence Wiley Professor, E-mail: hcchen@civil.tamu.edu

http://www.techno-press.org/?journal=ose&subpage=7 ISSN: 2093-6702 (Print), 2093-677X (Online)

navigation channel, the drift angles of the passing ships, the modes of passing ship coupling, and the shape and bathymetry of ship basins.

In the present study, the seabed bathymetry was reproduced as precisely as possible using the NOAA geophysical database for Virginia Beach, NOAA nautical charts for Hampton Roads and Norfolk harbor, and the echo sounding data for the navigation channel and waterfront facilities. The objective of the present work is to study the effects of all the other key parameters mentioned above at the specific site. In the simulation scenario, passing ships with prescribed constant speeds cruise in the specified ship lanes. The moored ship are restrained by mooring lines and cushioned by fenders from the piers, and allowed the freedom of surge, sway and yawing motions. The free surface effect is ignored as the motion responses of the moored ships are mainly from the surface pressure and shear stresses over the wetted hulls of the floating structures.

2. Methodology

In order to provide accurate resolution of the transient turbulent flows induced by the passing ships, it is necessary to solve the unsteady Reynolds-Averaged Navier-Stokes (RANS) equations:

$$U^i_{,i} = 0 \tag{1}$$

$$\frac{\partial U^i}{\partial t} + U^j U^i_{,j} + \left(\overline{u^i u^j}\right)_{,j} = -g^{ij} p_{,j} + \frac{1}{Re} g^{jk} U^i_{,jk} \tag{2}$$

where U^i and u^i represent the mean and fluctuating velocity components, and g^{ij} is conjugate metric tensor. t is time, p is pressure, and $Re = U_o L/\nu$ is the Reynolds number. The continuity Eq. (1) and mean momentum Eq. (2) are written in tensor notations with subscripts $_{,j}$ and $_{,jk}$ as the covariant derivatives.

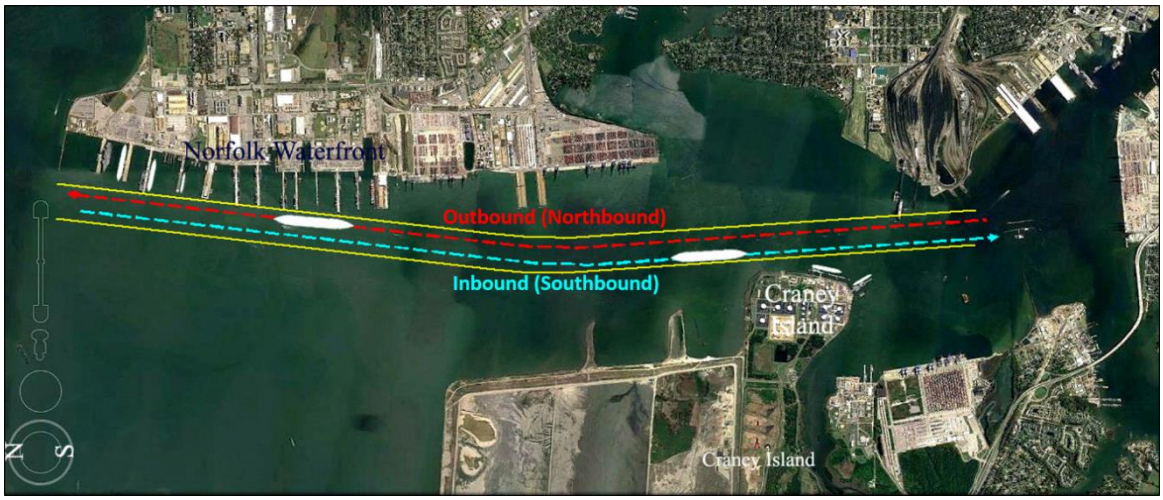

Fig. 1 Overview of simulation site

The Finite-Analytic Navier-Stokes (FANS) code developed by Chen, Patel and Ju (1990) and Pontaza, Chen and Reddy (2005) is employed for time-domain simulation of the passing ship effects. The FANS code solves the unsteady Navier-Stokes equations in conjunction with advanced near-wall turbulence models in general curvilinear coordinates and moving overset grids. The overset grid approach provides great flexibility in representing complex geometries and allows for judicial mesh refinements in the form of embedded or overlapping grids. The FANS code has been used extensively for the simulations of ship berthing operations and floating pier interactions (Chen and Huang 2003a, b), multiple-ship interaction in navigation channels (Chen *et al*. 2002a, b, c, Chen *et al.* 2003), and site-specific passing ship simulations (Huang and Chen 2003, 2006, 2007, 2010). For the present passing ship simulations, the two-layer turbulence model of Chen and Patel (1988) is employed to provide closure for the Reynolds stress tensor $\overline{u^i u^j}$.

To handle the ship and fender coupling dynamics, the FANS code is coupled with a Compound Ocean Structure Motion Analysis (COSMA) program developed by Huang (1990). COSMA was designed for the prediction of ship motions, fender loads, and mooring line tensions for each moored ship. For the present study, ships and pier are treated as rigid bodies, and the coupling members are fenders and mooring lines. COSMA uses a lumped mass-spring model to represent the structural responses and was originally for potential flow simulations. When coupled with a RANS code, both the added mass and damping forces are accounted for by the hydrodynamic forces $\{F_h\}$ calculated from the RANS solutions. The equation of motion implemented in COSMA can then be revised in the general form

$$[M]\{\ddot{X}(t)\}+[K+C]\{X(t)\}=\{F_h(t)\} \tag{3}$$

where $[M]$ is the generalized inertia matrix, $[K]$ the hydrodynamic restoring force coefficient matrix, $[C]$ the restoring coefficient due to coupling members, and $\{X(t)\}$ the generalized displacement vector.

For ship induced flows, FANS code is employed to calculate the transient flow field and the associated hydrodynamic forces $\{F_h(t)\}$. COSMA is then used to solve the displacement vector $\{X(t)\}$. Once the new ship position and the corresponding fender deflection are determined, the numerical grids for both the passing and moored ships can be updated using the moving overset grid approach. In this coupled process, COSMA is considerably more sensitive to the time step sizes than the FANS code, as the fender stiffness essentially limits the time increment for the motion code. To stabilize the motion responses, COSMA uses a reduced time increment of 1/20 of that of CFD simulations, which generally provides a good result. Note that this practice has little impact to the overall computation efficiency, as the COSMA code requires only a negligible fraction of the CPU time used by the FANS simulations.

3. Numerical model

3.1 Seabed bathymetry and waterfront topology

In order to capture the site-specific passing ship effects in the present simulations, the exact seabed bathymetry was reproduced using various database in public domain as of June 2017. This includes the NOAA database for Virginia Beach, the Norfolk harbor nautical charts, and the echo sounding data for the navigational channels, NAVSTA Norfolk waterfront, under-pier data,

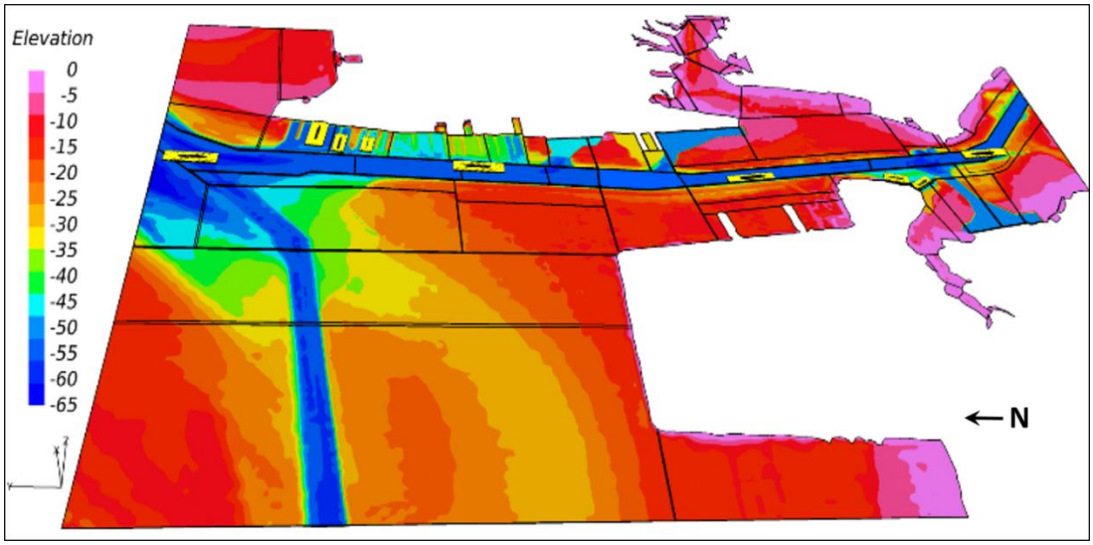

Fig. 2 Seabed bathymetry and initial ship positions

and Craney Island rehandling basin.

Major efforts were made to achieve the accurate seabed bathymetry in this project. Discrepancies among the available database were found and had to be reconciled. The procedure was outlined in Chen *et al.* (2018), thus not repeated in the present paper. It is suffice to mention that the initial seabed bathymetry was constructed with the NOAA database. The nautical chart and echo sounding data, showing several dredged basins not in NOAA database, were then incorporated to refine the seabed bathymetry to the utmost precision attainable for the navigation channel and waterfront facilities. Fig. 2 shows the detailed seabed bathymetry for the computational domain, including both NAVSTA Norfolk and Craney Island Fuel Terminal. The *x*- and *y*-axes are chosen to point to the east and north, respectively. Note that outbound is northbound and inbound means southbound for the passing ships.

3.2 Facility layouts and model ship selection

The passing ships selected for the present study are Gen 3 MSC Daniela containerships with overall length (between perpendiculars) L = 1,201ft, beam 168 ft, and draft 51.2 ft. As the exact ship geometry is not available, a similar type of Suezmax containership (length = 1,242 ft, beam = 180 ft, and draft = 46.9 ft) was reshaped to match the particulars of the MSC Daniela ship. There are three moored ships at NAVSTA Norfolk with DDG ship at Pier 10, LHD ship at Pier 11, and CVN ship at Pier 12, as depicted in Fig. 3. Two identical oiler ships (AOEc and AOEd) are moored at Piers C and D at Craney Island, as shown in Fig. 4. Summary of the ship particulars is listed in Table 1. Client ships are secured to their piers with mooring lines to prevent excessive drifting under the influence of passing ships and cushioned by fenders. The mooring and fender stiffness are tuned to achieve reasonable motion responses of the moored vessels in the worst-case scenario of this study.

It is viable to simulate the entire area engaging all four passing ships and five moored ships using the FANS code. However, little is gained as the two facilities in consideration are too far

apart for interference between the two sites. It is also more complex to design a single simulation matrix covering two distinctively different sets of passing ship scenarios at the NAVSTA Norfolk and Craney Island sites with different channel width, channel orientation, and pier configurations. It is therefore more convenient to split the present simulation scenarios in two domains, as depicted in Figs. 3 and 4, with sufficient overlaps to ensure proper flow propagation. The computational domain for the NAVSTA Norfolk site consists of 53 grid blocks (49 computational blocks and 4 phantom blocks) with a total of 10,124,676 grid points. The Craney Island domain is covered by 100 grid blocks (95 computational blocks and 5 phantom blocks) to provide accurate resolution of the complex bank line geometry. The total grid at the Craney Island site is smaller with 7,372,131 nodes, since the navigation channel narrows from 1,200 ft at NAVSTA to 800 ft here, and the water depth is rather shallow away from the channel banks.

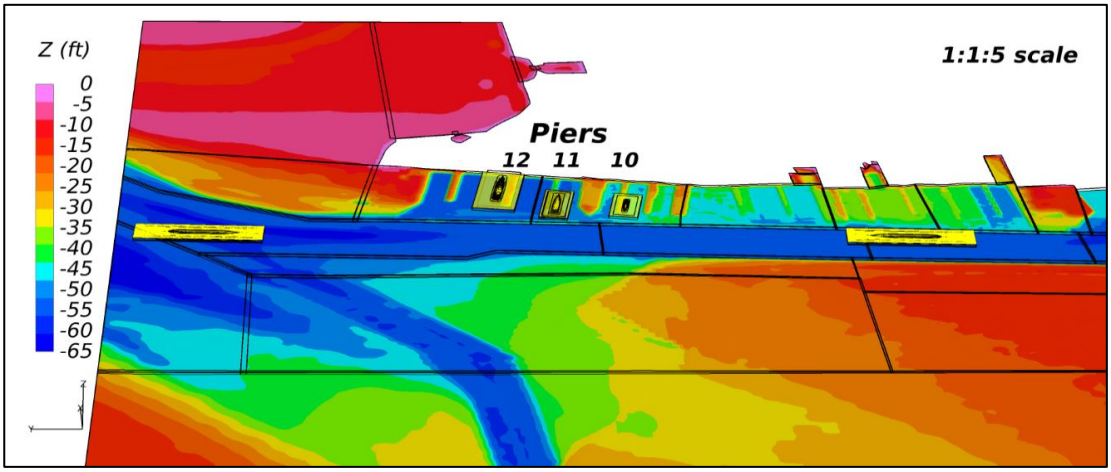

Fig. 3 Ship layout for the NAVSTA Norfolk study

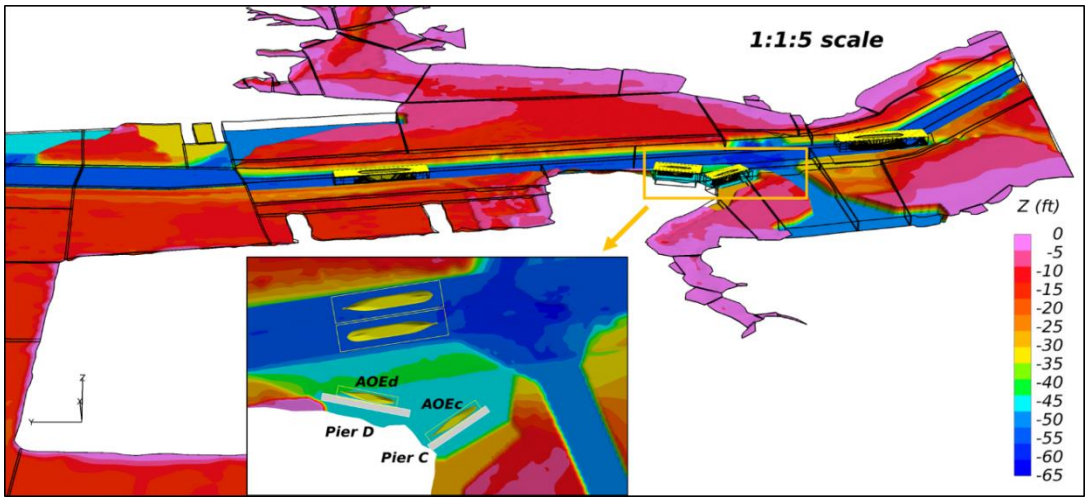

Fig. 4 Ship layout for the Craney Island study

Table 1 Summary of ship particulars

	Passing Ships	**Moored Ships**			
		DDG	**LHD**	**CVN**	**AOE**
L*wl* (m)	366 (1,201 ft)	142.04	237.13	318	223
Beam (m)	51.2 (168 ft)	20.12	32.31	41	32.6
Draft (m)	15.6 (51.2 ft)	9.45	8.23	11.6	11.6
Mass (tons)	-	8,270	41,950	87,920	49,600
Izz (ton*m^2)	-	1.4E7	3.7E8	7.4E8	2.0E8

Table 2 Summary of simulation cases for NAVSTA Norfolk site. Ship lanes are measured from the channel east bank

Case No.	**Speed (kt)**		**Ship Lane (ft)**	
	IB	**OB**	**IB**	**OB**
Group 1: core parametric study with two passing ships				
1-5	11	11	684	100, 120, 200, 300, 450
6-10	9	9	684	100, 120, 200, 300, 450
11-15	7	7	684	100, 120, 200, 300, 450
16-20	5	5	684	100, 120, 200, 300, 450
Group 2: core parametric study with an outbound passing ship				
21-25	-	11	-	100, 120, 200, 300, 450
26-30	-	9	-	100, 120, 200, 300, 450
31-35	-	7	-	100, 120, 200, 300, 450
36-40	-	5		100, 120, 200, 300, 450
Group 3: additional runs with an outbound passing ship to verify trend of lane effects				
41-43	-	7	-	140, 160, 180
Group 4: an inbound ship heading south in various lanes				
44-47	7	-	100, 200, 300, 450	-
48-51	5, 7, 9, 11	-	684	-
Group 5: effect of 5-degree drift angle for an outbound ship				
52	-	7	-	300 (5°W)
53	-	7	-	300 (5°E)
Group 6: overtaking encounter of two ships in same direction				
54	-	E9, W5	-	E300, W684
55	-	E5, W9	-	E300, W684
56	E9, W5	-	E300, W684	-
57	E5, W9	-	E300, W684	-
Group 7: to identify the worst case scenario of head-on encounter (inline separation distance *S* with ship length *L* = 1,201 ft)				
58-67	5, 7	5, 7	684	300 (*S*/*L* = 7, 8, 9, 10, 11)
68	7	7	684	200 (*S*/*L* = 10)
69-73	11	11	684	100, 120, 200, 300, 450 (*S*/*L* = 10)
74	11	11	684	300 (*S*/*L* = 11)

The orientation of the moored ship relative to the navigation channel is another interesting factor on the passing ship effects. The client ships at NAVSTA Norfolk are moored along piers nearly perpendicular to the channel, as illustrated in Fig. 3. Fig. 4 shows the two oiler ships at Craney Island at large skew angles relative to the navigation channel. The narrower navigation channel at Craney Island also means closer proximity of the passing ships to the moored ships, thus more pronounced effects are expected.

3.3 Selection of simulation cases

In the present study, a complete test matrix including 112 simulation cases (57 for NAVSTA Norfolk and 55 for Craney Island) of coupled motion analysis was carried out for various combinations of ship lanes and passing ship speeds, water depths, drift angles, and passing ship couplings (head-on or overtaking encounter). Furthermore, a series of pilot simulations were a priori to the core parametric study to identify the worst-case scenario of ship coupling effects under the head-on encounter conditions.

Table 2 gives the test matrix for the NAVSTA Norfolk site with 57 cases of coupled CFD and

Table 3 Summary of simulation cases for Craney Island site. Ship lanes are measured from the channel west bank

Case No.	Speed (kt)		Ship Lane (ft)	
	IB	**OB**	**IB**	**OB**
Group 1: core parametric study with two passing ships				
1-4	11	11	100, 150, 200, 300	484
5-8	9	9	100, 150, 200, 300	484
9-12	7	7	100, 150, 200, 300	484
13-16	5	5	100, 150, 200, 300	484
Group 2: core parametric study with an inbound passing ship				
17-20	11	-	100, 150, 200, 300	-
21-24	9	-	100, 150, 200, 300	-
25-28	7	-	100, 150, 200, 300	-
29-32	5	-	100, 150, 200, 300	-
Group 3: additional runs with an inbound passing ship to verify trend of lane effects				
33-36	7	-	125, 175, 250, 484	-
Group 4: an outbound ship heading north in various lanes				
37-40	-	7	-	100, 200, 300, 450
41-44	-	5, 7, 9, 11	-	484
Group 5: reference cases at current channel depth of 52 feet (reduce ship draft by 3 feet)				
45-49	7	-	100, 150, 200, 300, 484	-
50-53	5	-	100, 150, 200, 300	-
Group 6: effect of 5-degree drift angle for an inbound ship				
54	7	-	300 (5°W)	-
55	7	-	300 (5°E)	-
Group 7: to identify the worst case scenario of head-on encounter (inline separation distance S with ship length L =1,201 ft)				
56-60	7	7	200 (S/L =7, 8, 9, 10, 11)	484
61-64	11	11	100, 150, 200, 300 (S/L = 10)	484
65	5	5	200 (S/L = 10)	484

ship motion analyses. All ship lanes are measured from the channel east bank, where the moored ships are located. All simulations are for the proposed dredged channel depth of 55 ft. OB stands for the outbound (northbound) ship, while IB represents the inbound (southbound) one. Group 1 consists of 20 core parametric studies with two passing ships in 5 ship lanes (100, 120, 200, 300, 450) ft at 4 different speeds (5, 7, 9, 11) knots. Group 2 involves the same 20 core parametric cases with an outbound passing ship alone. Group 3 includes 3 additional runs with an outbound ship to verify the trend of lane effects at (140, 160, 180) ft. Group 4 studies the effect of an inbound ship in various ship lanes or at different speeds. Group 5 examines the effect of drift angle for an inbound passing ship at +5° and −5° drift angles. Group 6 consists of overtaking of either two inbound ships or two outbound ones. Ship speeds and lanes are labeled by E for the ship in the east side and W in the west. Group 7 includes 17 pilot simulations to identify the worst-case scenario.

Table 3 shows the test matrix for the Craney Island site with 55 cases of passing ship studies. Ship lanes for this site are measured from the channel west bank, where the two moored ships are located. Unless specified otherwise, all simulations are for the proposed dredged channel depth of 55 ft. Group 1 investigates 16 core parametric cases with two passing ships in 4 ship lanes (100, 150, 200, 300) ft at 4 different speeds (5, 7, 9, 11) knots. Group 2 involves the same 16 core parametric studies with an inbound passing ship alone. Group 3 includes 4 additional runs with an inbound ship to verify the trend of lane effects at (125, 175, 250, 484) ft. Group 4 studies the effect of an outbound ship in various ship lanes or at different speeds. Group 5 consists of 9 reference cases for one inbound passing ship at the current channel depth of 52 ft. Group 6 examines the effect of drift angle for an inbound passing ship at +5° and −5° drift angles. Group 7 consists of 10 pilot simulations to identify the worst-case scenario.

The characteristic length was chosen to be 1,000 ft and the characteristic velocity 5 kt in the FANS code. All simulations were performed with no-slip conditions on the sea floor and the harbor and river banks. Neumann boundary conditions were specified on all open boundaries of the computational domain. The free surface effect was neglected as the highest Froude number for the passing ships was below 0.0945. This allowed us to specify zero vertical velocity, and zero gradients for horizontal velocities, pressure, and turbulence quantities on the free surface.

4. Simulation results and discussion: NAVSTA Norfolk site

All simulations for this site were performed using 20 cores (CPUs) on the Ada cluster at Texas A&M Supercomputing Facility. A maximum wall-clock time of 24 hours was specified, and most simulations were completed in 19-22 hours.

4.1 Identification of worst-case scenario at NAVSTA Norfolk

The worst-case scenario, with the largest hydrodynamic forces and/or moments induced by the passing ships during head-on encounters, must be identified in order to design the mooring and fender stiffness for the moored vessels and the initial positions of the passing ships. To explore the effect of the encounter position, the initial position of the inbound (southbound) ship is kept constant, while that of the outbound (northbound) ship is placed with various inline separation distances. A total of 17 head-on encounter simulations (Cases 58-74 in Table 2) with different combinations of encounter locations and ship speeds were carried out to determine the highest hydrodynamic loading on the stationary moored ships.

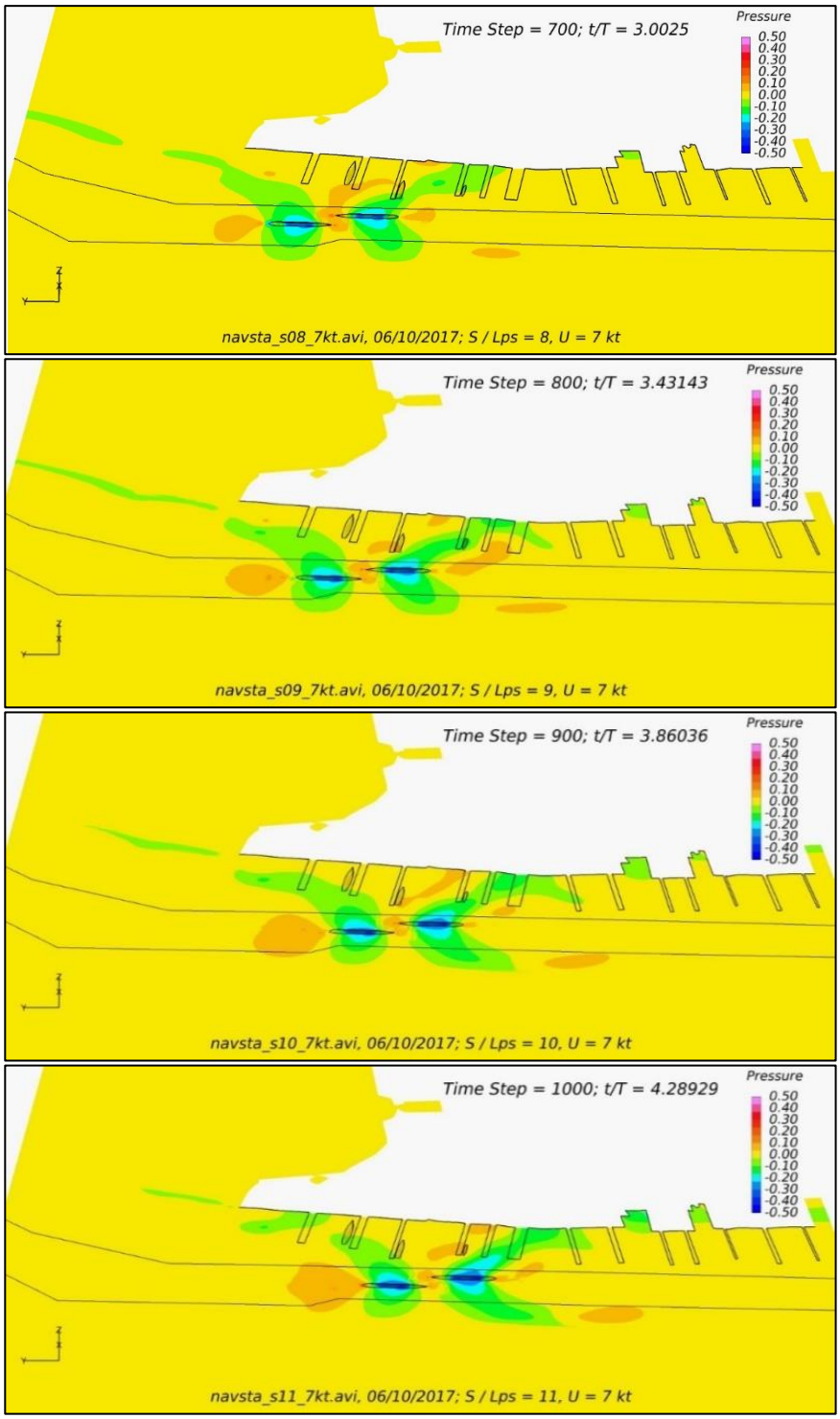

Fig. 5 Comparison of pressure contours with two passing ships in head-on encounter positions with *S/L* = 8, 9, 10, 11

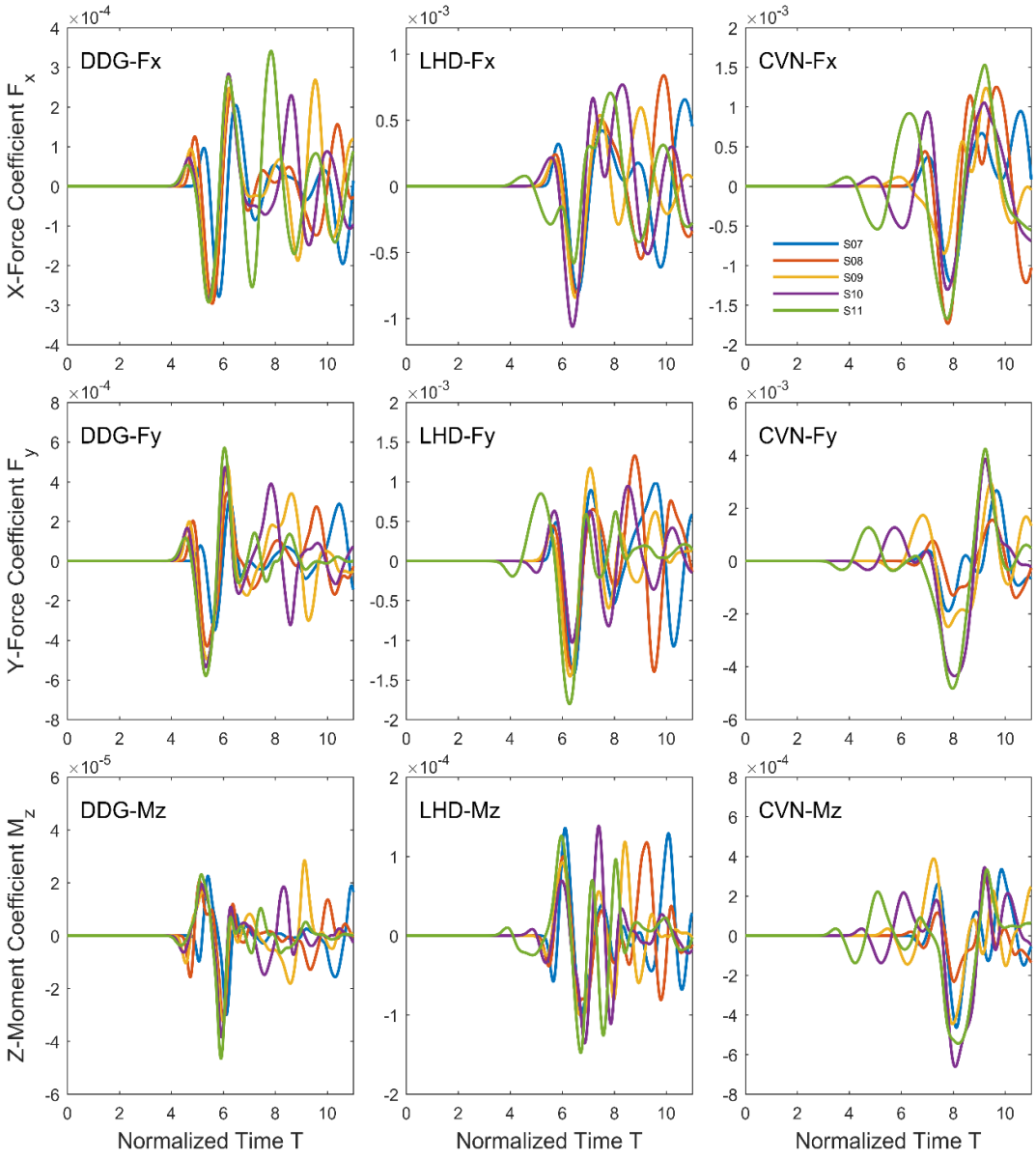

Fig. 6 Effect of head-on encounter locations on the DDG, LHD, and CVN ships

Fig. 5 showcases the pressure contours for U = 7 kt at 4 different encounter positions with *S/L* = 8, 9, 10, and 11, where *S* is the initial separation distance (CG to CG) between the inbound and outbound ships, and *L* = 1,201 ft is again the length of the passing ships. Obviously, the closer the head-on ships encounter position to a moored ship, the stronger its impact of the passing ship effects. It was determined that *S/L* = 10, with the inbound and outbound ships passing each other

near Pier 11, as the most suitable selection for all three moored ships. In view of this, the core parametric studies (Cases 1-53 in Table 2) were performed with the outbound ship positioned 12,010 ft from the inbound one initially.

The corresponding time histories of hydrodynamic forces and moments on the DDG, LHD, and CVN ships are plotted in Fig. 6 at five encounter positions with *S/L* = (7, 8, 9, 10, 11). Fig. 6 uses a normalized time, such that the peak forces/moments appear around the same time for easy comparison. The dimensionless forces F_x and F_y given in Fig. 6 are in the global *x*– and *y*–directions. However, the forces in the following sections are transformed into the ship local coordinates as the surge and sway forces. Fig. 6 also shows *S/L* = 10 as a good choice of the encounter position, producing either peak or near peak hydrodynamic forces and moments for all three ships.

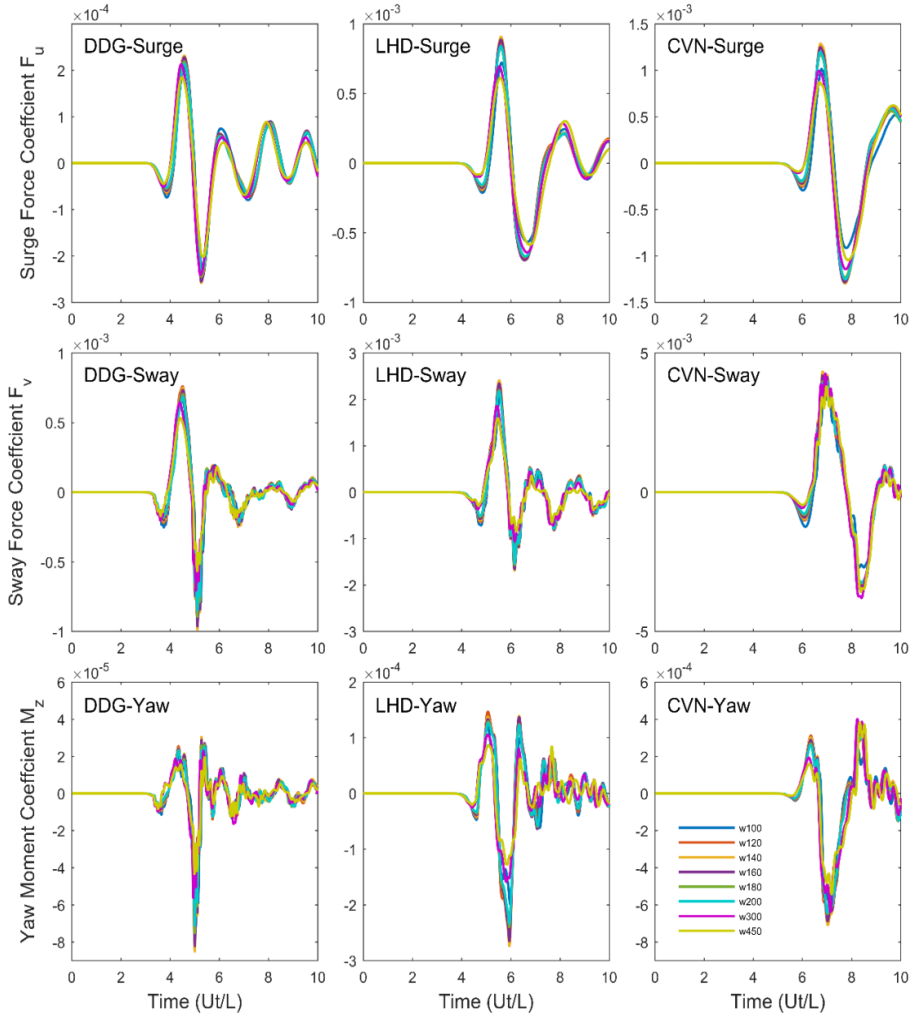

Fig. 7 Surge and sway forces and yaw moments induced by a 7 kt outbound ship in 8 different ship lanes

4.2 Outbound ship at NAVSTA Norfolk

A total of 23 simulations were performed to investigate the passing ship effects induced by an outbound ship at NAVSTA Norfolk. In the core parametric study of Group 2, coupled FANS/COSMA simulations were carried out for 5 different ship lanes, w = (100, 120, 200, 300, 450) ft, and 4 different ship speeds, U = (5, 7, 9, 11) kt, as listed in Cases 21-40 of Table 2. Three additional simulations (Cases 41-43) were also performed in Group 3 for ship lanes w = (120, 140, 160) ft to refine the search of the worst case with the highest hydrodynamic loads induced by the outbound passing ship.

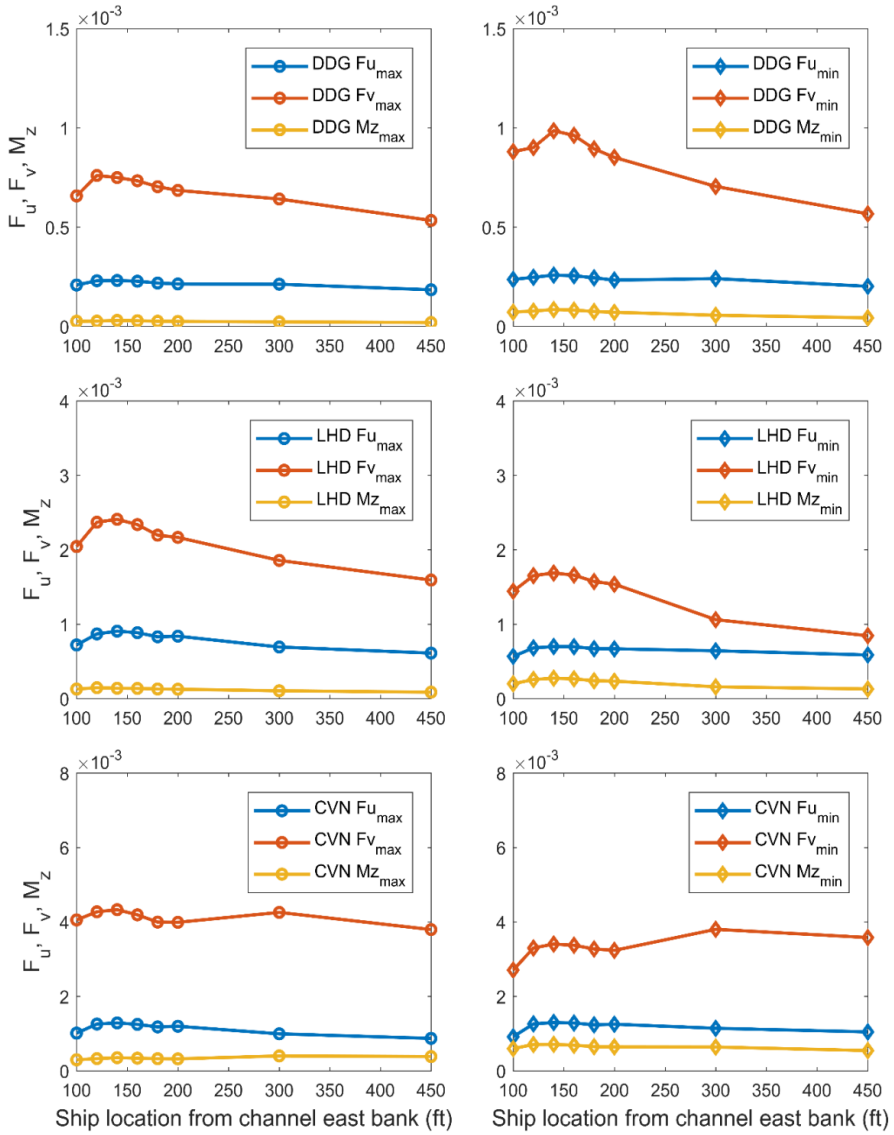

Fig. 8 Peak forces and moments induced by a 7 kt outbound ship in 8 different ship lanes

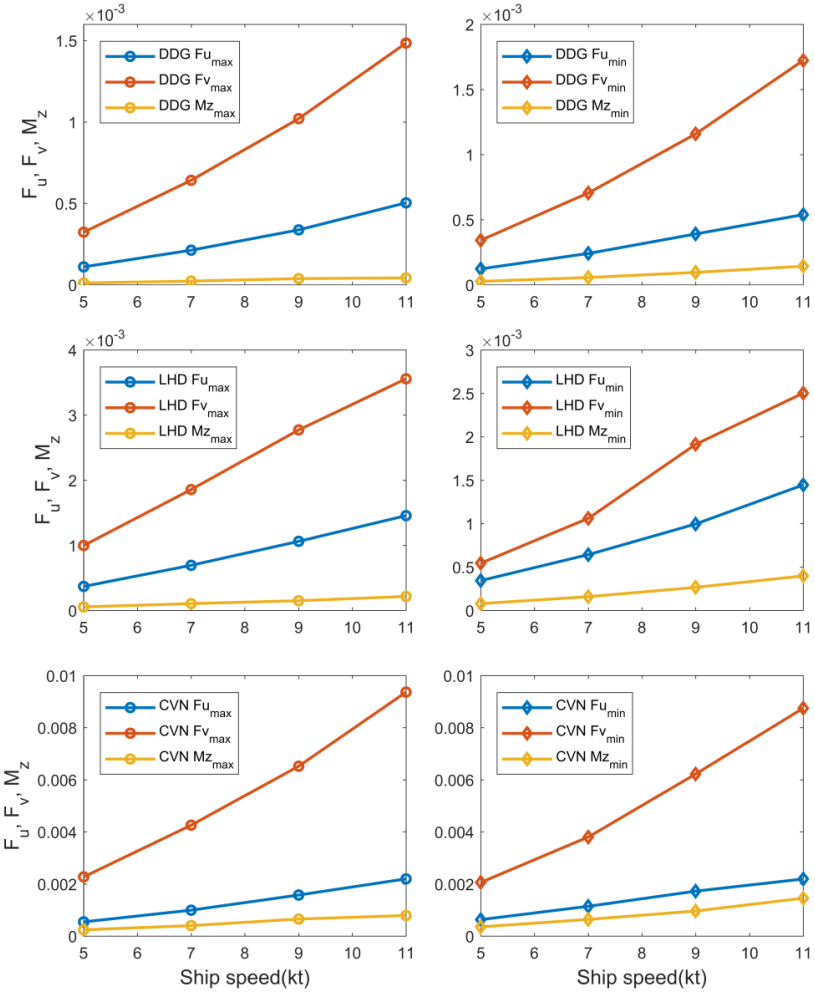

Fig. 9 Peak forces and moments induced by a outbound ship at 4 different speeds

Time histories of surge and sway forces, and yaw moment on the three moored ships induced by the 7 kt outbound ship are given in Fig. 7. Fig. 8 shows that the peak (maximum and minimum) forces and moments occur around w = 140 ft for the DDG and LHD ships. The pattern of the peak sway force is somewhat different for CVN, possibly affected by its farther distance from the navigation channel, the site-specific waterfront configuration and the pressure reflection by the quay wall.

The effect of the passing ship speed on the moored ships is illustrated in Fig. 9. Although the induced pressure for a stationary object should be roughly proportional to U^2 for high Reynolds number flows, the rate is lower than U^2 for a moored ship. This is because the fender reaction forces and mooring line tensions do not scale up quadratically with the passing ship speed. Both

the head-on ships and the inbound ship cases also show similar ship speed effect and will not be mentioned again.

4.3 Inbound ship at NAVSTA Norfolk

A total of 8 simulations were performed to evaluate the effects of ship lane and ship speed in the case of an inbound passing ship. Fig. 10 shows the forces and moments induced by the inbound passing ship at 7 kt. The corresponding peak forces plotted in Fig. 11 clearly indicate a monotonic ship lane effect.

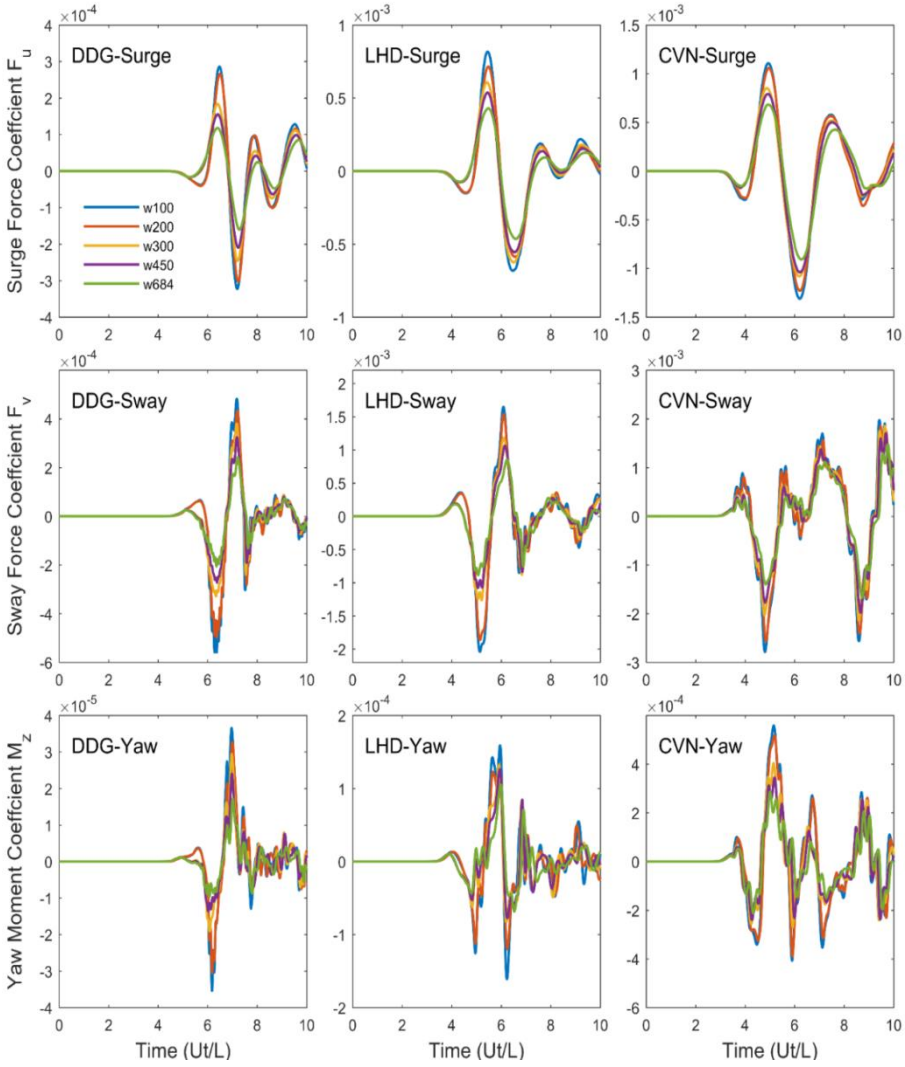

Fig. 10 Surge and sway forces, and yaw moments induced by a 7 kt inbound ship in 5 different ship lanes

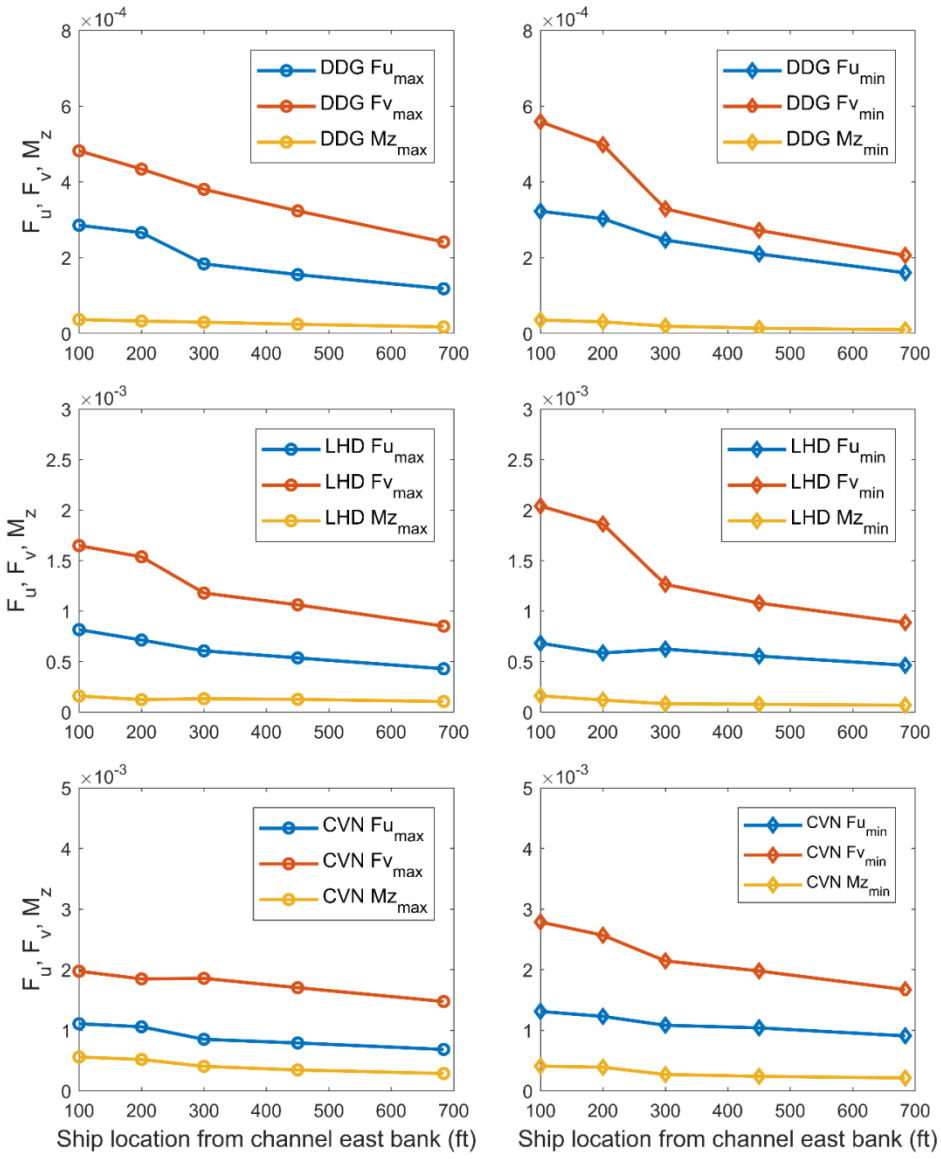

Fig. 11 Peak forces and moments induced in 5 different ship lanes

This trend is consistent with the passing ship effects in an open water basin with constant water depth. It can be seen in Fig. 3 that the water depth around Piers 10-12 is nearly uniform and the elevation change from the basin to the navigation channel is relatively small. Consequently, the channel bank effect during the initial stage of the inbound ship excursion is much weaker than that of the outbound ship in the same ship lane.

4.4 Effect of drift angle for outbound ship at NAVSTA Norfolk

For ships traveling in cross winds, it is necessary to turn the ship bow against the wind in order to maintain a straight course. Figs. 12 and 13 present the simulation results for a 7 kt outbound ship at different drift angles under east wind, calm wind, and west wind conditions. Apparently the passing ship induces higher hydrodynamic forces and yaw moments under the east wind condition, with the ship bow turning toward the waterfront.

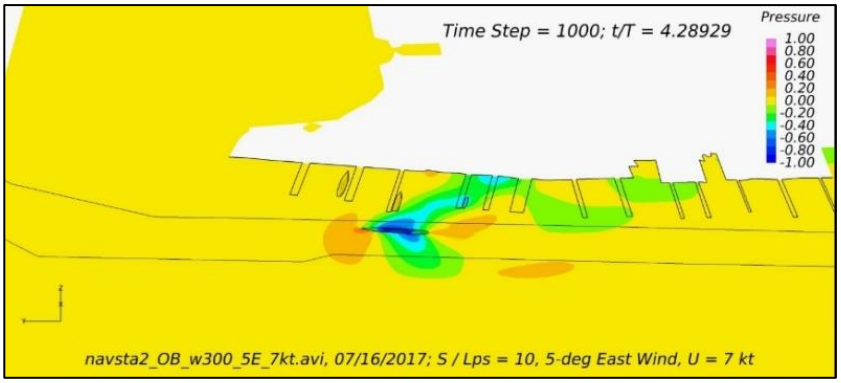

(a) East wind

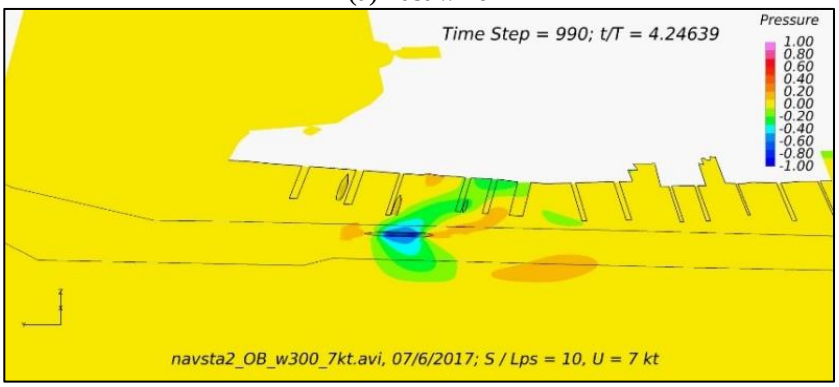

(b) Calm wind

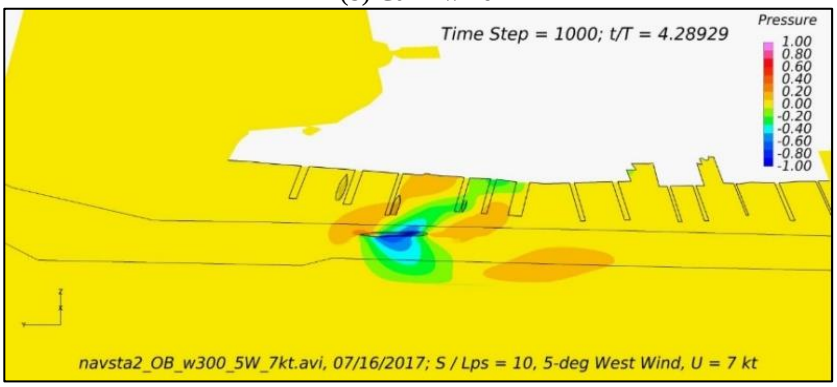

(c) West wind

Fig. 12 Pressure fields induced by a 7 kt outbound ship with different draft angles

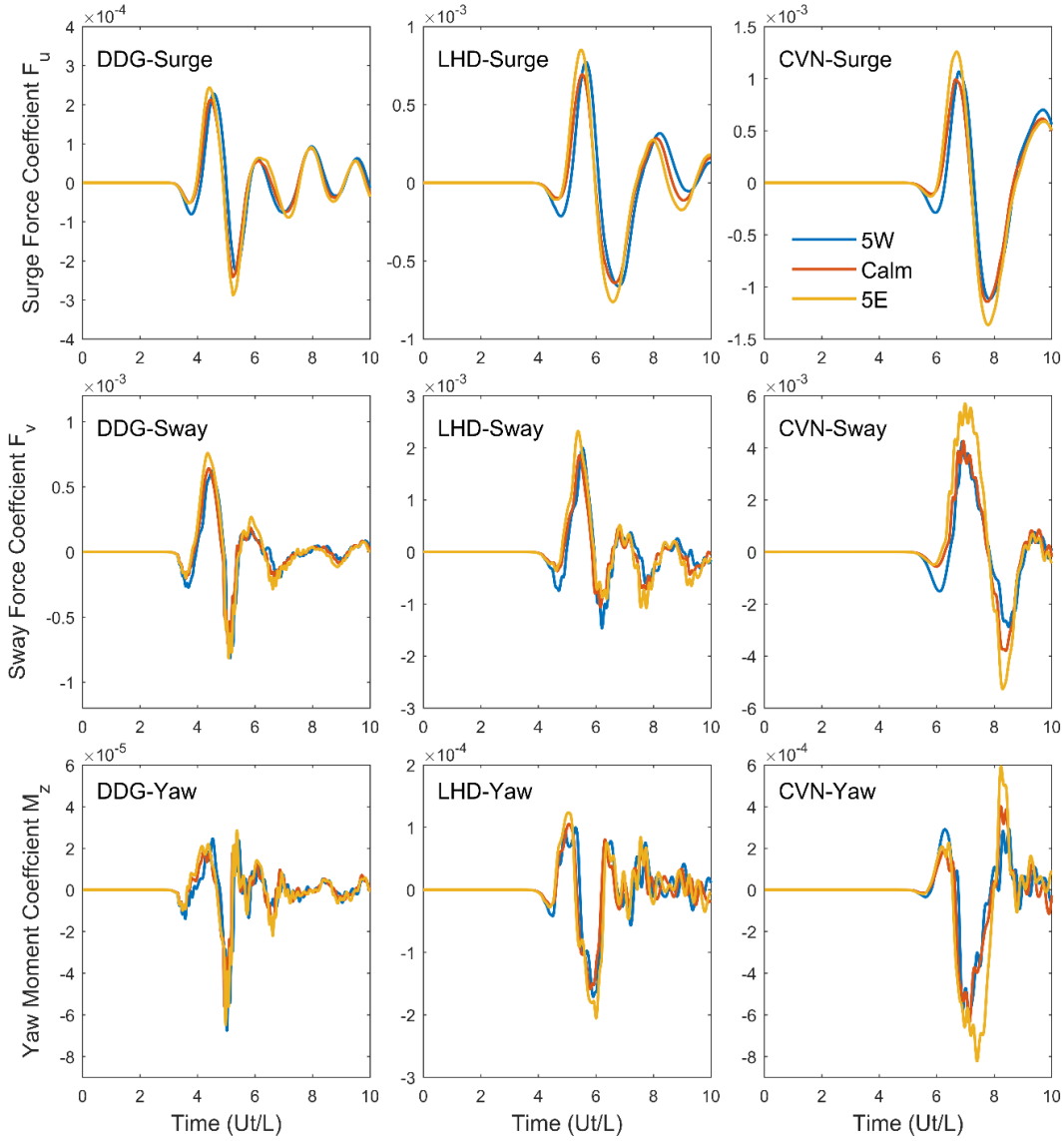

Fig. 13 Surge and sway forces, and yaw moments induced by an outbound ship at different drift angles

As the ship bow turns toward the channel bank, the flow passage around the bow area is reduced and generates an increase of suction pressure, which then propagates to the moored ships. When the ship bow turns away from the waterfront under the west wind condition, the bow-induced suction pressure is observed in the open water area away from the waterfront, with only minor influences on the moored ships. Therefore, the force and moment magnitudes under the calm wind and west wind conditions are about the same.

4.5 Two passing ships in head-on encounter at NAVSTA Norfolk

As listed in Group 1 of Table 2, 20 simulations were carried out in the head-on passing ships study. In these simulations, the inbound ship stays in the same ship lane of w = 684 ft, while the outbound ship moves from ship lane of w =100 ft to w = 450 ft. The minimum separation distance (sidewall to sidewall) between the two ships reduces from 416 ft to 66 ft, producing a dramatic increase of the ship coupling effect.

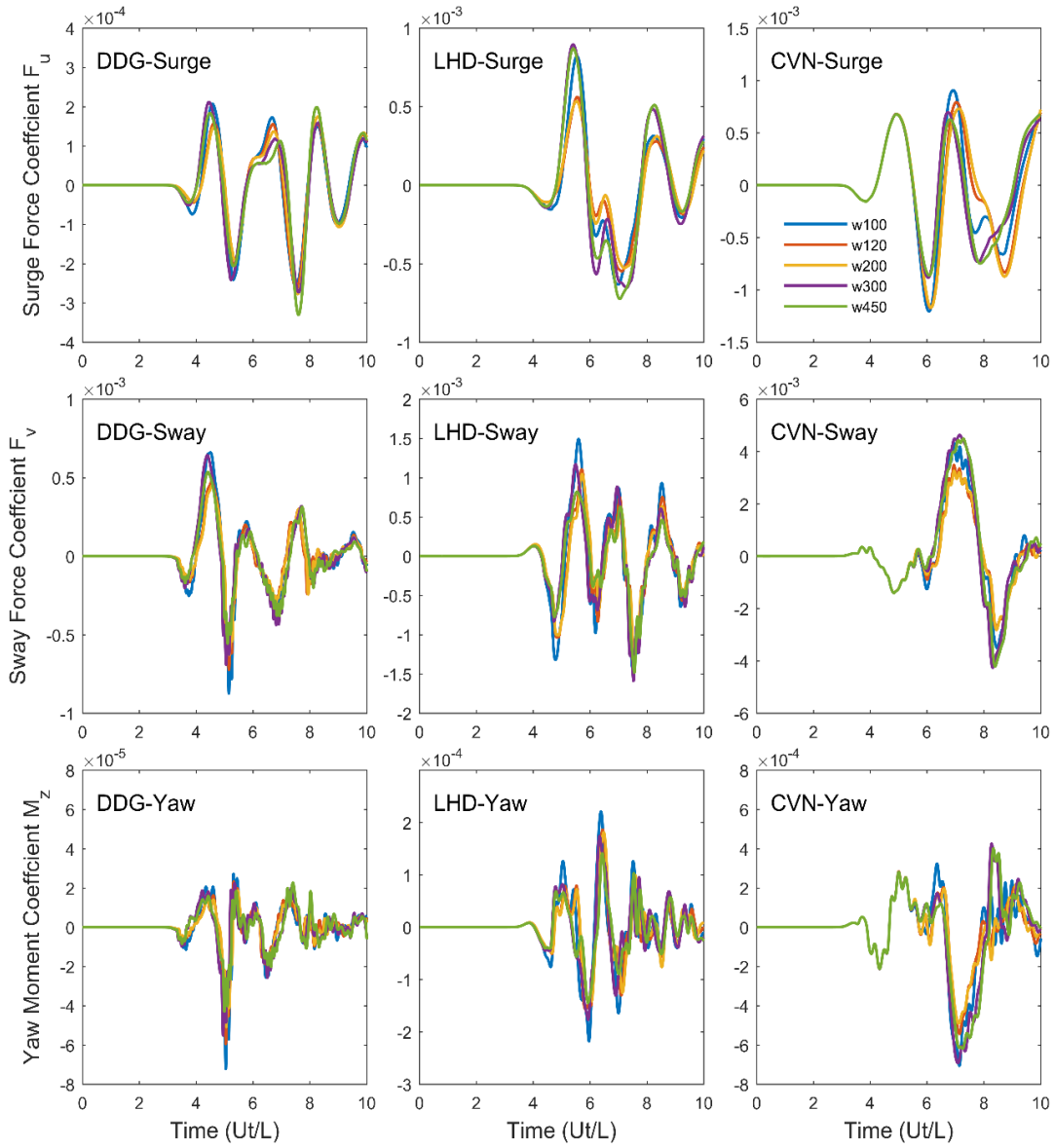

Fig. 14 Effect of ship lanes for passing ships in head-on encounter

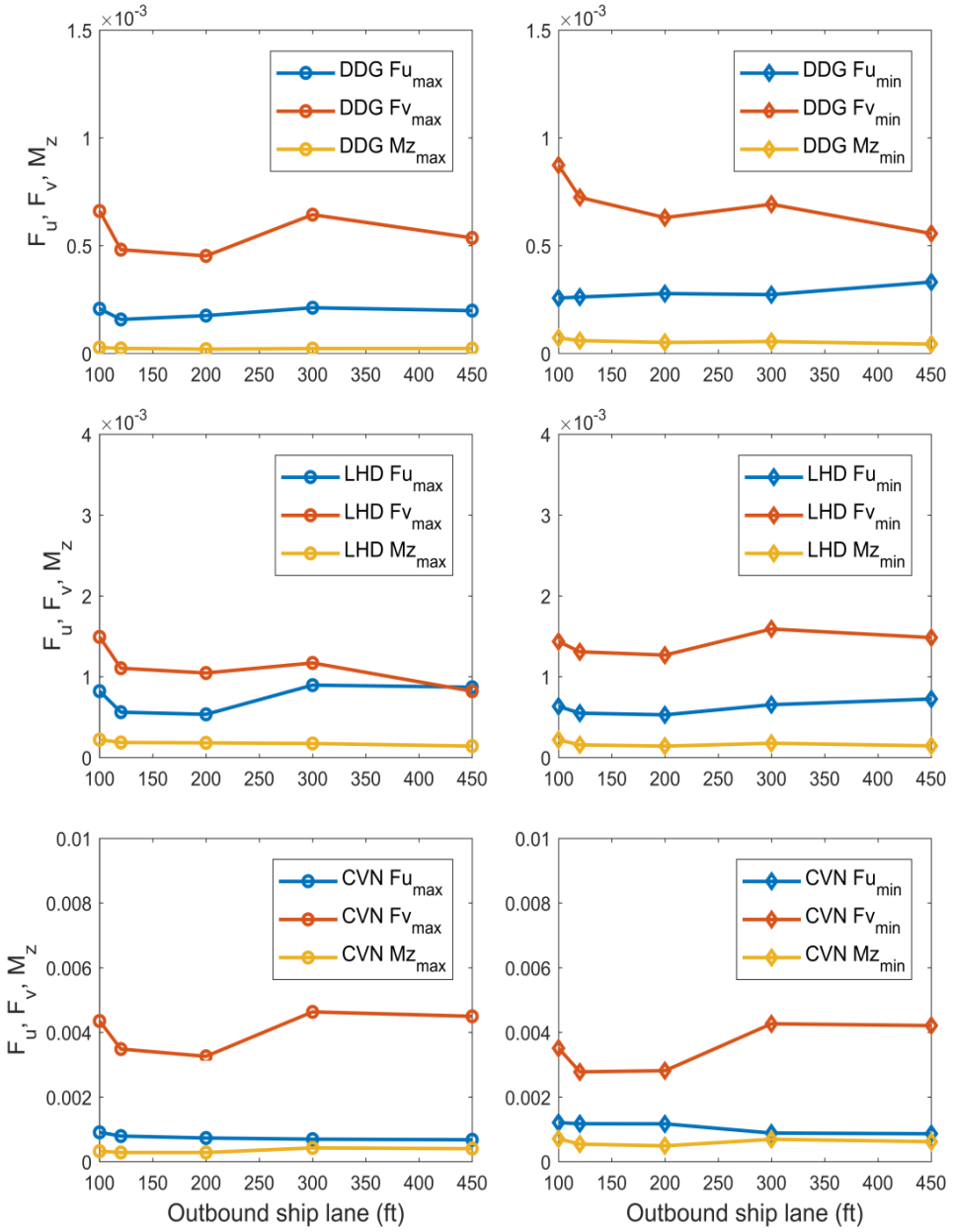

Fig. 15 Peak forces and moments induced in head-on encounter

Fig. 14 shows the ship lane effect of the surge and sway forces, and yaw moments on the moored ships induced by two 7 kt head-on ships. The ship lane effect is more complex than the single passing ship cases, not only from the combined influences of the passing ships, but also

showing the sheltering effect between them. Fig. 15 gives the corresponding peak hydrodynamic forces and moments. Both the sway and surge curves are not monotonic and much flatter than those in Fig. 11. This suggests strong sheltering effect in head-on encounter scenario, thus weak ship lane effect.

4.6 Overtaking encounter at NAVSTA Norfolk

Another ship coupling effect, with two passing ships in overtaking encounter, was investigated as listed in Group 6 of Table 2. Fig. 16 shows the pressure fields for two outbound ships in overtaking encounters with both ships heading north. In Case 54 the east ship travels at 9 kt and overtakes the west ship traveling at 5 kt. The ship speed is reversed for Case 55, with the faster west ship at 9 kt overtaking the east ship at 5 kt. In both cases, the total excursion distance of the faster ship is 10 ship lengths (i.e., $S/L = 10$), while the slower ship travels 5.5556 ship lengths over the same duration. The slower ship starts at 2.2222 L ahead of the faster ship, and the overtaking occurs at the same location as the head-on encounter (near LHD ship at Pier 11). The forces and moments histories on the moored ships are displayed in Fig. 17, along with the single outbound ship at 9 kt case for comparison. It can be concluded that the effect of the overtaking encounter is dominated by the faster ship, and in general it induces higher forces and moments than the single passing ship at the higher speed. However, the sheltering effect can also be observed in the sway force of the CVN ship. Similar results are found for two inbound ships in overtaking encounter.

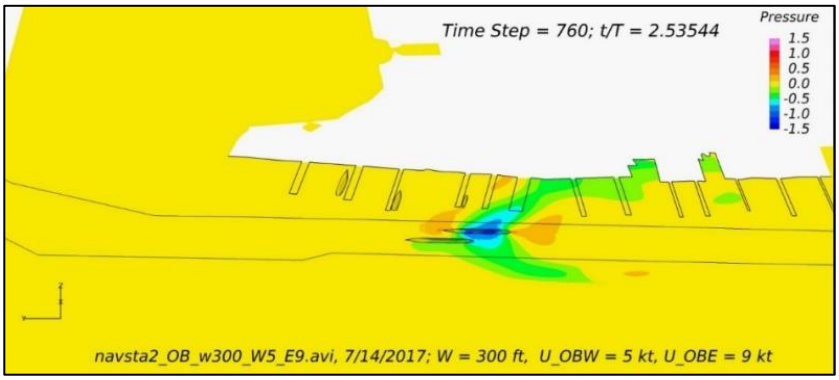

(a) East Ship at 9 kt Overtaking West Ship at 5 kt

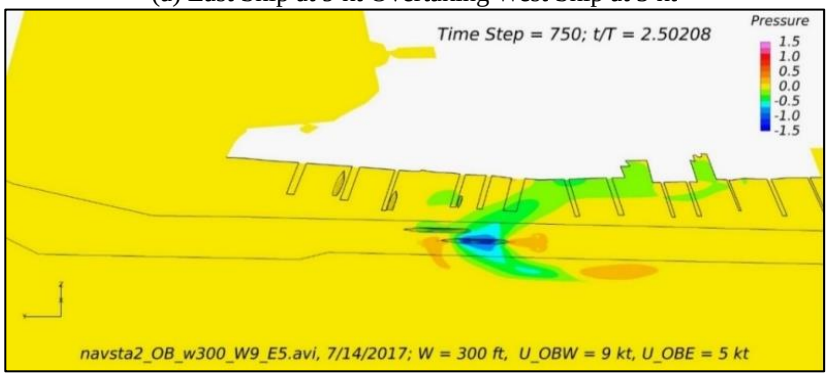

(b) West Ship at 9 kt Overtaking East Ship at 5 kt

Fig. 16 Pressure fields induced by two outbound ships in overtaking encounter

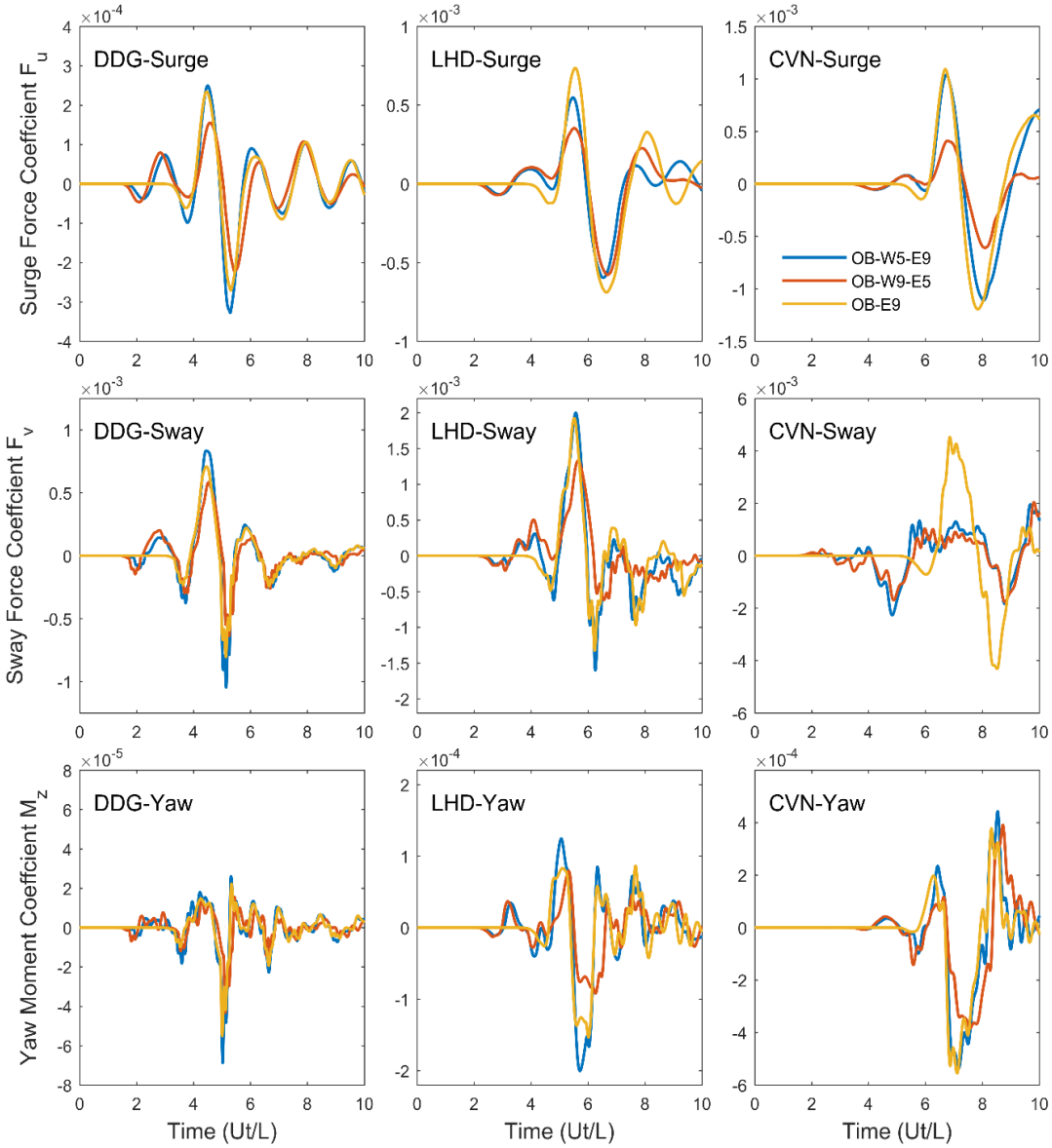

Fig. 17 Hydrodynamic forces and moments induced by two outbound ships in overtaking encounter

5. Simulation results and discussion: Craney Island site

All simulations, except those in section 5.2, are for the proposed dredged channel depth of 55 ft. Simulations with two passing ships were performed using 17 CPUs on the Texas A&M Ada cluster. Those with only one passing ship can be accomplished with 15 CPUs. Most simulations were completed in 20-22 hours.

5.1 Identification of worst-case scenario at Craney Island

As seen in Fig. 4, the Craney Island site is close to the southern end of the navigation channel where the channel makes a sharp turn towards southeast. Certain measures were taken to ensure the passing ships would not need to cruise beyond the channel bend under different head-on encounter scenarios. Therefore, only the initial position of the inbound ship was adjusted to achieve the different encounter position. Two adjustments to the ship speeds were also made to avoid the need for the ships to negotiate the channel bend and still achieve the desired encounter positions. The outbound ship was initially placed at the channel bend and given a ramp start, meaning its speed increased linearly to the designed speed, for the first 400 time steps ($0 < t < 2$). Similarly, the inbound ship was given a linear ramp stop for the last 600 time steps. For Case 60 in Table 3 with separation distance $S/L = 11$, the total excursion distance of the outbound ship is 11 L, and 10.5 L for the inbound one. A total of 10 head-on encounter simulations (Cases 56-65 in Table 3) with different combinations of encounter location and ship speed were performed to determine the highest hydrodynamic loading acting on the two stationary moored ships. The information was then analyzed to design the initial positions of the passing ships, as well as the mooring and fender stiffness for the moored vessels.

Fig. 18 showcases the pressure contours for U = 7 kt at four encounter positions with S/L = 8, 9, 10 and 11. The hydrodynamic forces and moments induced on the two moored ships are shown in Fig. 19 for all 5 encounter positions, with the same time normalization defined in section 4.1. The force and moment histories indicate that the AOEc ship experiences a single peak similar to open water conditions, as it is moored nearly perpendicular to the Craney Island shorelines with negligible pressure reflections. By contrast, the AOEd ship is strongly affected by the shorelines, with multiple peaks and valleys in hydrodynamics forces induced by the passing ships. The study of the force and moment histories suggests the worst-case scenario at $S/L = 10$, with the inbound and outbound ships passing each other near the AOEd ship at Pier D. Based on this, the core parametric study of two passing ships in head-on encounter (Cases 1-16 in Table 3) will be performed with an initial separation distance of 12,010 ft (i.e., $S/L = 10$).

It is interesting to note the Craney Island topology plays a role in the simulations. By examining the pressure contours, it is clear the Craney Island land mass blocks the pressure fields induced by the inbound ship until it gets close to Pier D. The AOEc ship is especially insensitive to the head-on encounter position studied, and its hydrodynamics forces are dominated by the pressure fields induced by the outbound ship.

5.2 Reference cases with inbound ship at Craney Island

Though the core test matrix is for the proposed channel depth of 55 ft, an investigation of the channel depth effect was made with the existing channel depth of 52 ft (Group 5 in Table 3) to establish the reference cases. Note the draft of the inbound passing ship was reduced from 51.2 ft to 48.2 ft to maintain the same under-keel clearance. The time histories and peak (maximum and minimum) magnitudes of forces and moments on the moored ships are presented in Figs. 20 and 21. These two figures indicate monotonically decreasing passing ship effects with increasing lateral distance from the west bank of the navigation channel. This suggests that the channel bank effect is relatively small under the present channel depth of 52 ft. Note that AOEc experienced the peak surge force an order of magnitude smaller than that of AOEd, because of its location and orientation.

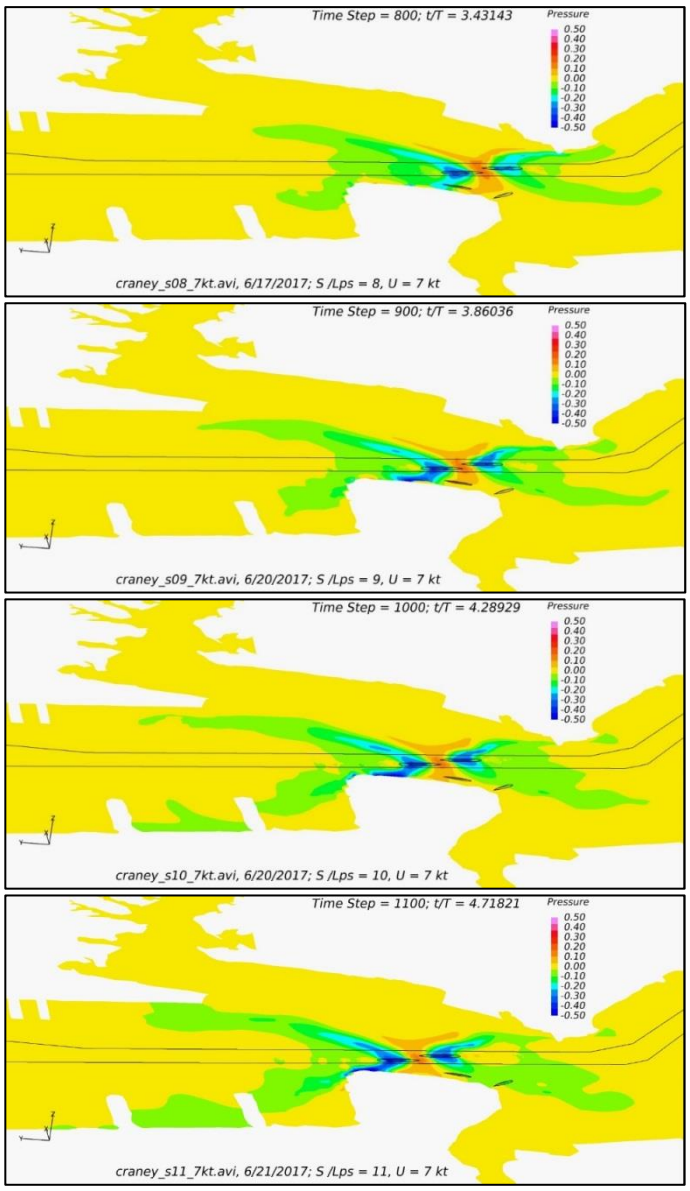

Fig. 18 Comparison of pressure contours with two passing ships in head-on encounter positions with *S/L* = 8, 9, 10, 11

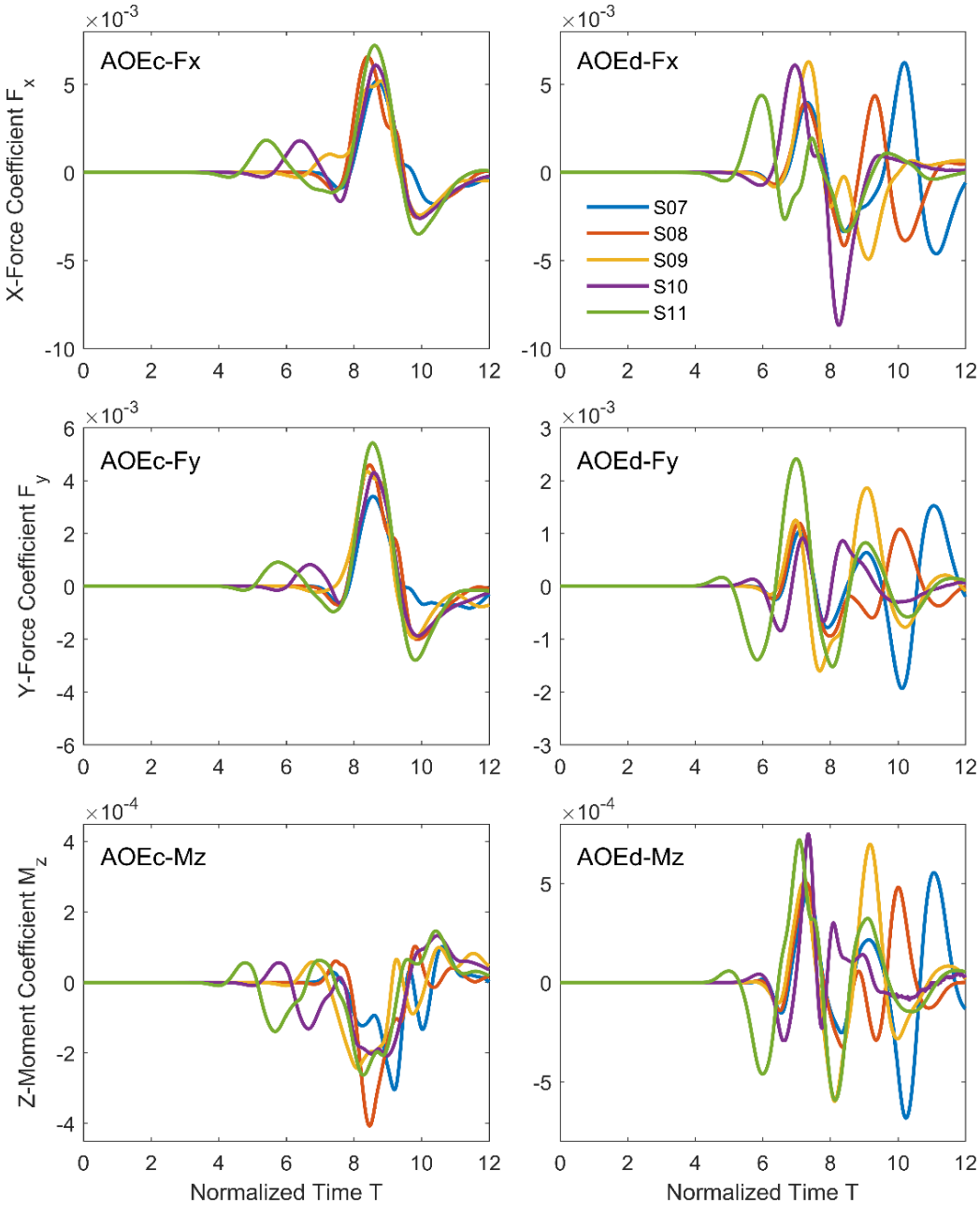

Fig. 19 Effect of head-on encounter locations on AOEc and AOEd ships

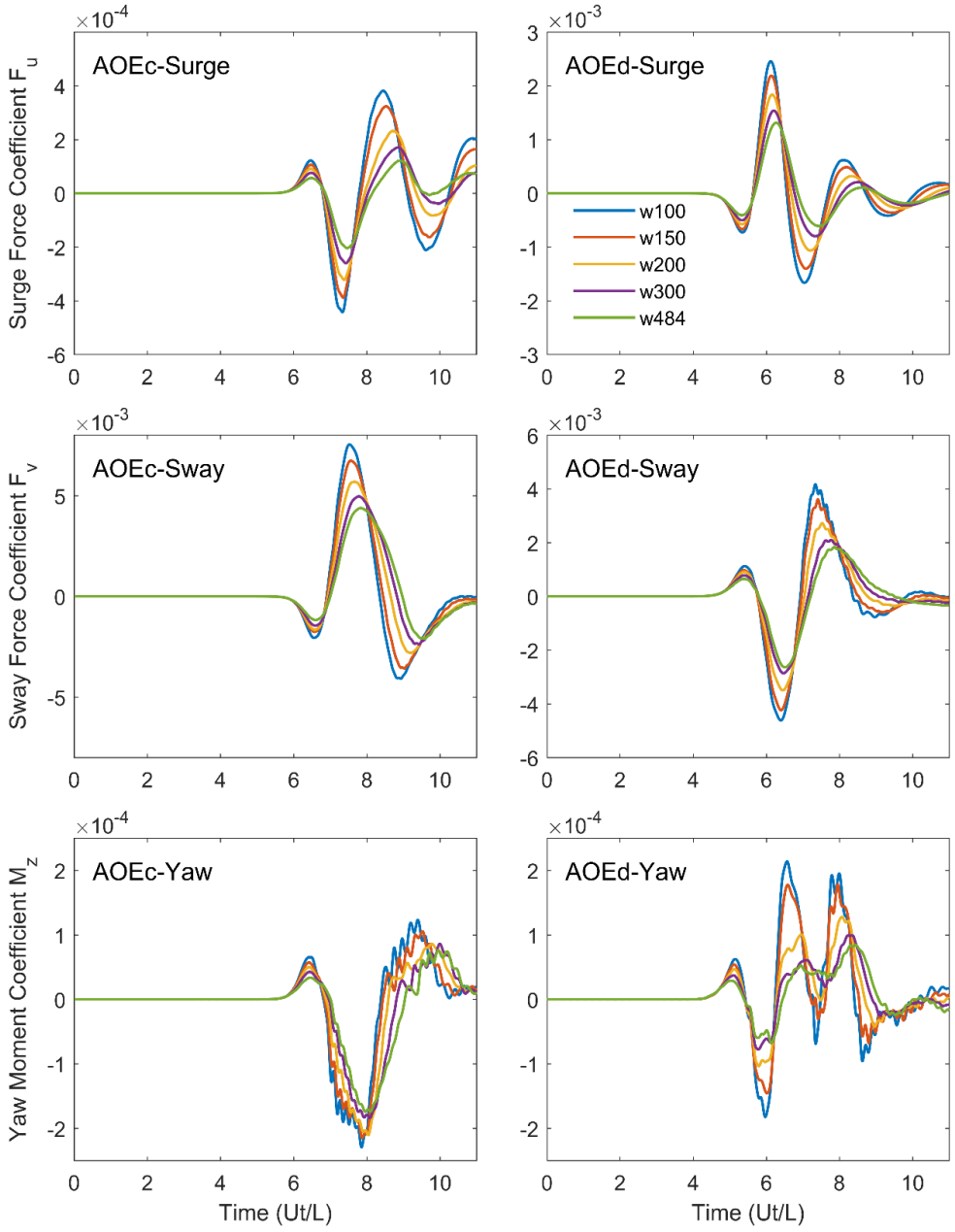

Fig. 20 Force and moment histories induced by a 7 kt inbound ship with the existing channel depth of 52 ft

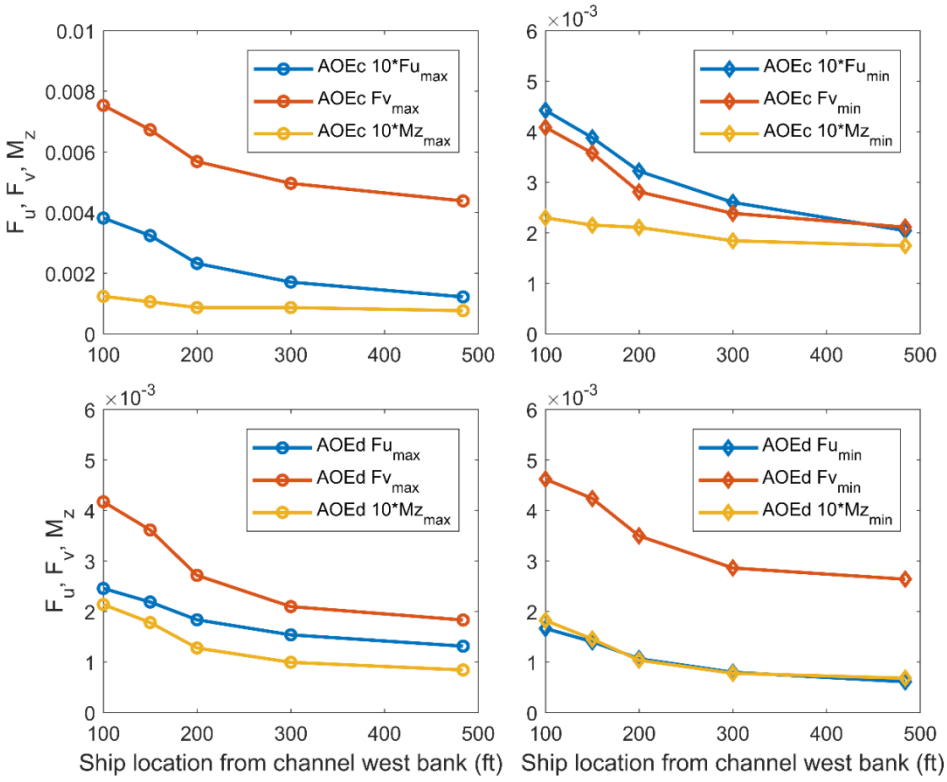

Fig. 21 Peak Forces and moments induced by a 7 kt inbound ship with the existing depth of 52 ft

5.3 Inbound ship at Craney Island

A total of 20 simulations (Cases 17-36 in Table 3) were carried out to investigate the passing ship effects induced by an inbound ship for the proposed 55 ft-deep channel. After the 16 core parametric studies in Group 2 with 4 different ship lanes of w = (100, 150, 200, 300) ft and 4 different ship speeds of U = (5, 7, 9, 11) kt, four additional simulations were performed in Group 3 for ship lanes of w = (125, 175, 250, 484) ft to refine the search of the worst-case with highest hydrodynamic loads induced by the inbound ship.

The time histories and peak magnitudes of forces and moment induced by a 7 kt inbound ship are given in Figs. 22 and 23. Compared to those under the existing conditions in Fig. 21 for the same ship lanes, both the force and moment histories exhibit very similar patterns but with significantly higher magnitudes. The larger hydrodynamic forces and moments are caused primarily by an increase of ship draft from 48.2 ft to 51.2 ft, which results in larger block coefficient for the passing ship. Fig. 23 shows that the induced peak forces and moments occur around w = 125 ft for both AOE ships. This phenomenon may be attributed to the confinement of the channel bank with water depth changing abruptly from 55 ft to 44 ft or less outside the navigation channel.

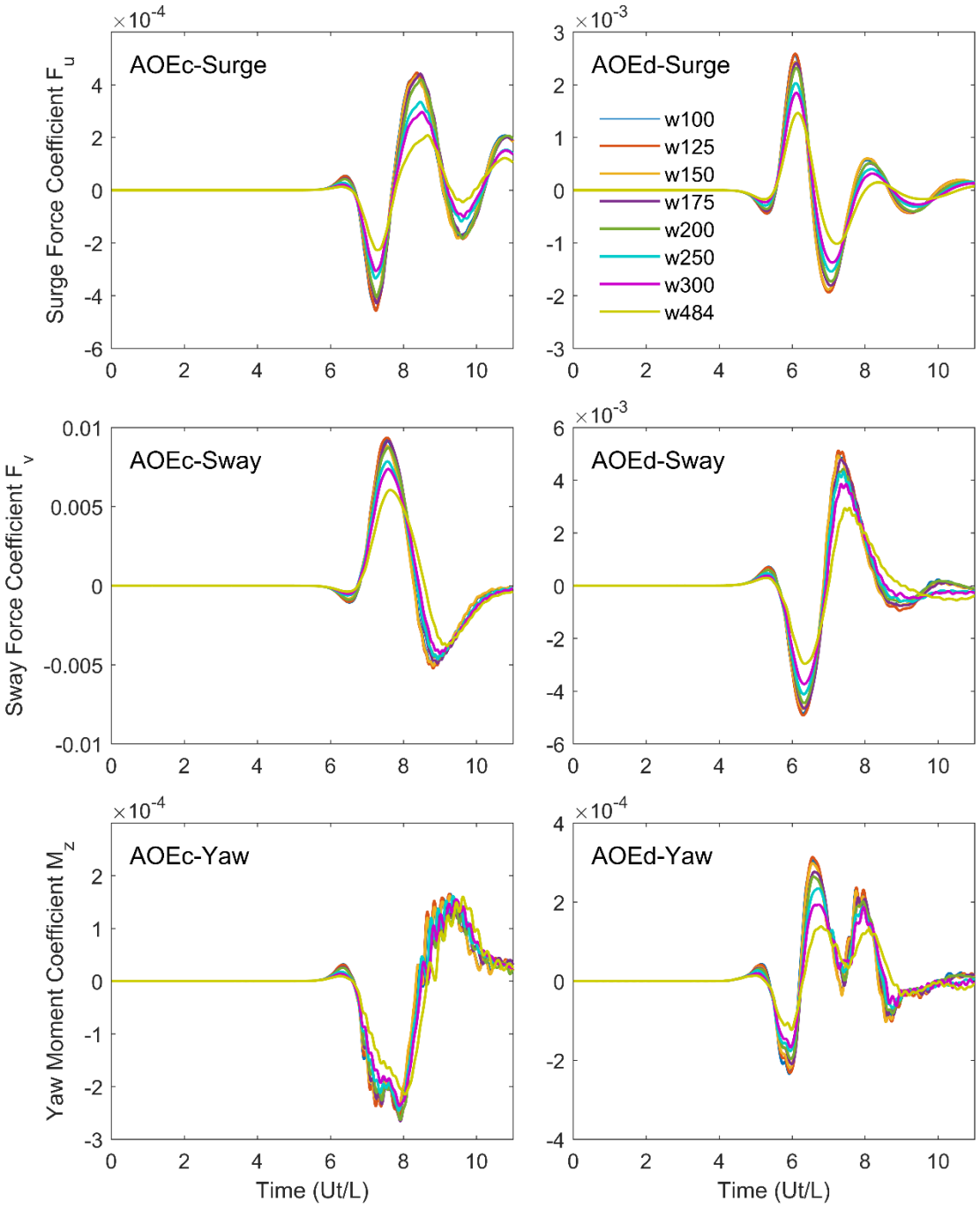

Fig. 22 Surge and sway forces, and yaw moments induced by a 7 kt inbound ship in 8 different ship lanes

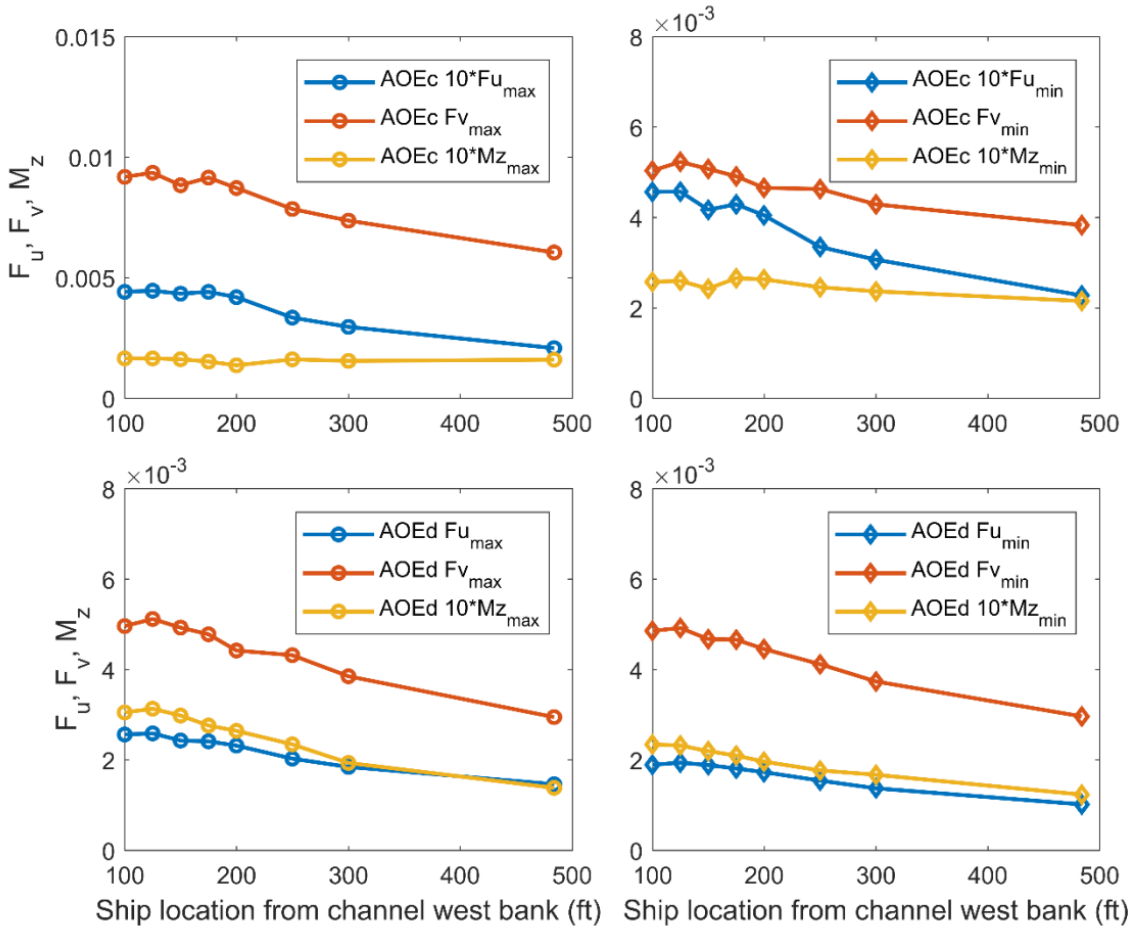

Fig. 23 Peak Forces and moments induced by a 7 kt inbound ship

A conclusion on the channel depth effect can be drawn by comparing the results in sections 5.2 and 5.3. While the channel bank effect is insignificant with the current channel depth of 52 ft, it is noticeable at the proposed dredging depth of 55 ft, assuming the same under-keel clearance. Also, the general trend of the ship speed effect at Craney Island is found to be similar to those observed at the NAVSTA Norfolk site, so it will not be mentioned below.

5.4 Outbound ship at Craney Island

A total of 8 simulations (Group 4 of Table 3) were performed to evaluate the effects of ship lane and ship speed induced by an outbound ship. Fig. 24 shows the forces and moment histories on the moored ships induced by an outbound ship at 7 kt in 5 different ship lanes. It is noted that the peak forces and yaw moment occur at w = 150 ft, similar to that observed for the inbound ship scenario.

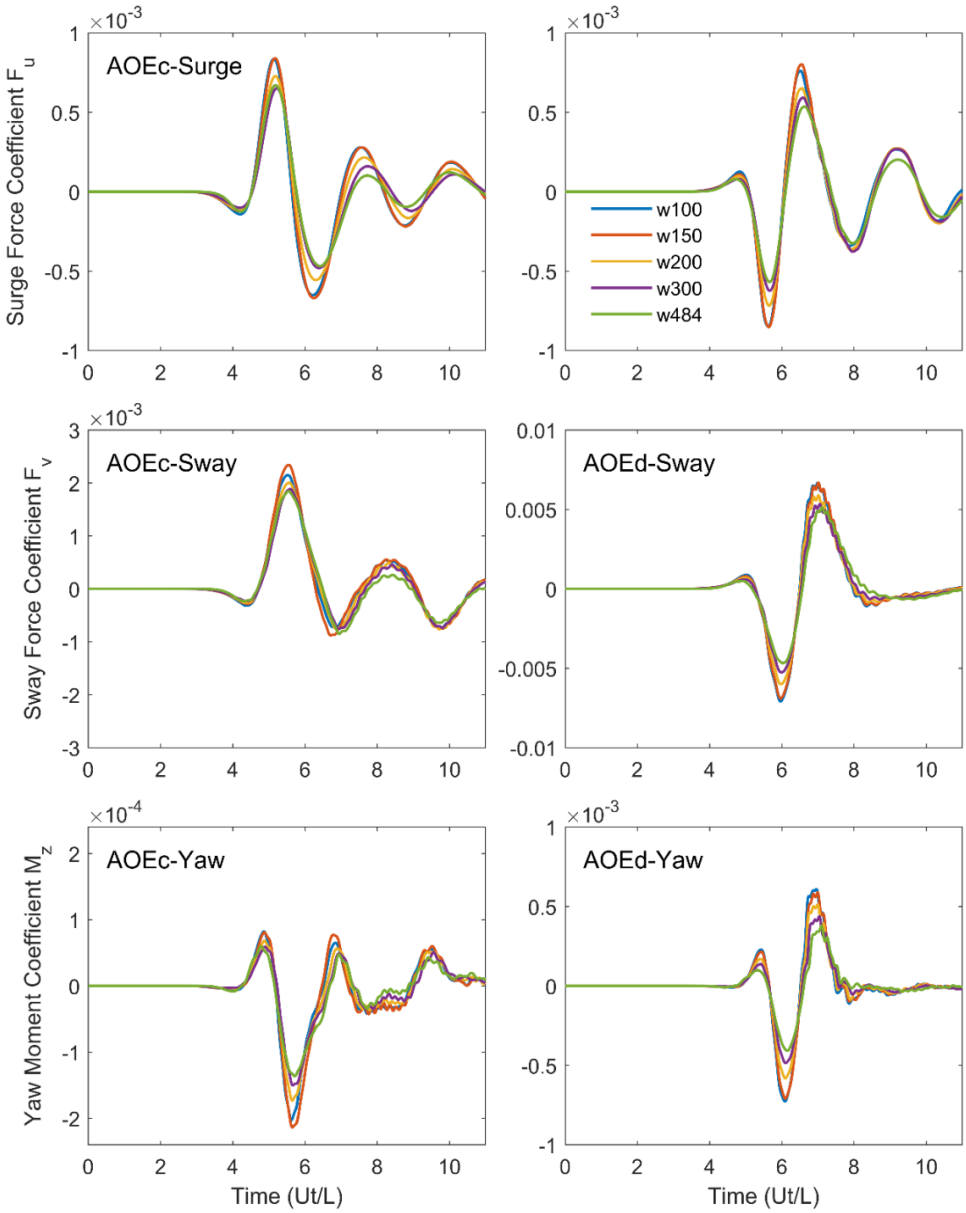

Fig. 24 Forces and moments induced by an outbound ship at 7 kt in 5 different ship lanes

5.5 Effect of drift angle for inbound ship at Craney Island

Figs. 25 and 26 present the simulation results of an inbound ship at different drift angles under west wind, calm wind, and east wind conditions. Fig. 26 indicates clearly that the passing ship induces higher hydrodynamic forces and yaw moments under the west wind condition, with the

ship bow turning toward the Craney Island waterfront. On the other hand, the calm wind and east wind conditions generate about the same force magnitudes. Similar to the phenomenon described in section 4.4, as the ship bow turns toward the waterfront facilities, it generates an increase of suction pressure propagating toward the moored ships. When it turns away from the waterfront under the east wind condition, the bow-induced suction pressure is observed in the open water area away from the waterfront, with only minor influences on the moored ships.

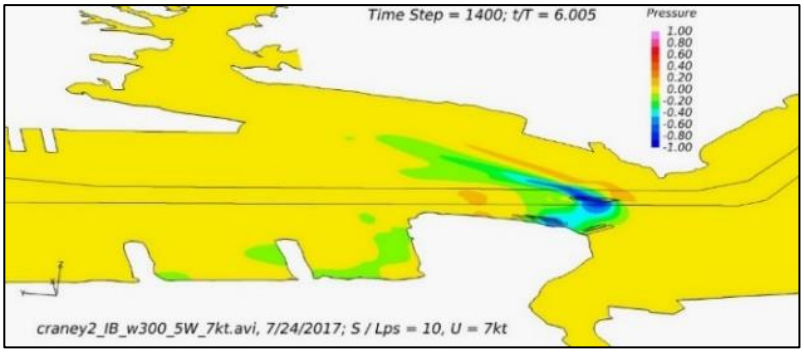

(a) West Wind

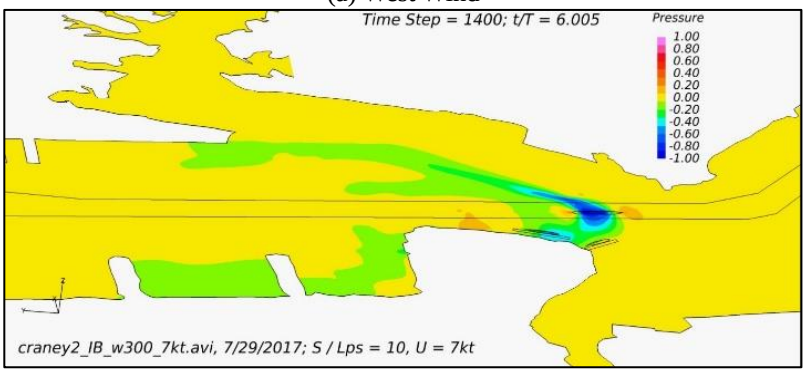

(b) Calm Wind

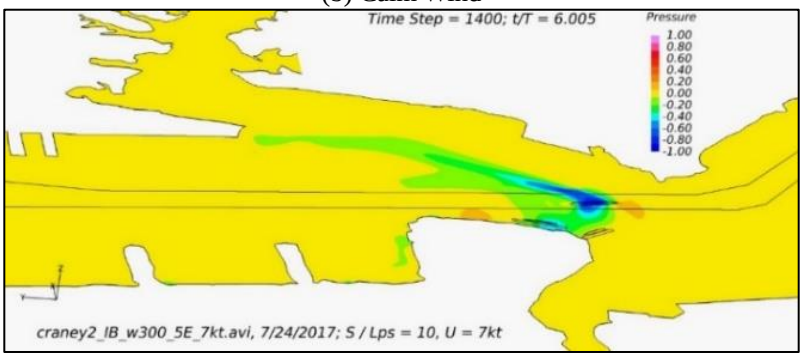

(c) East Wind

Fig. 25 Pressure fields induced by an inbound ship with different draft angles

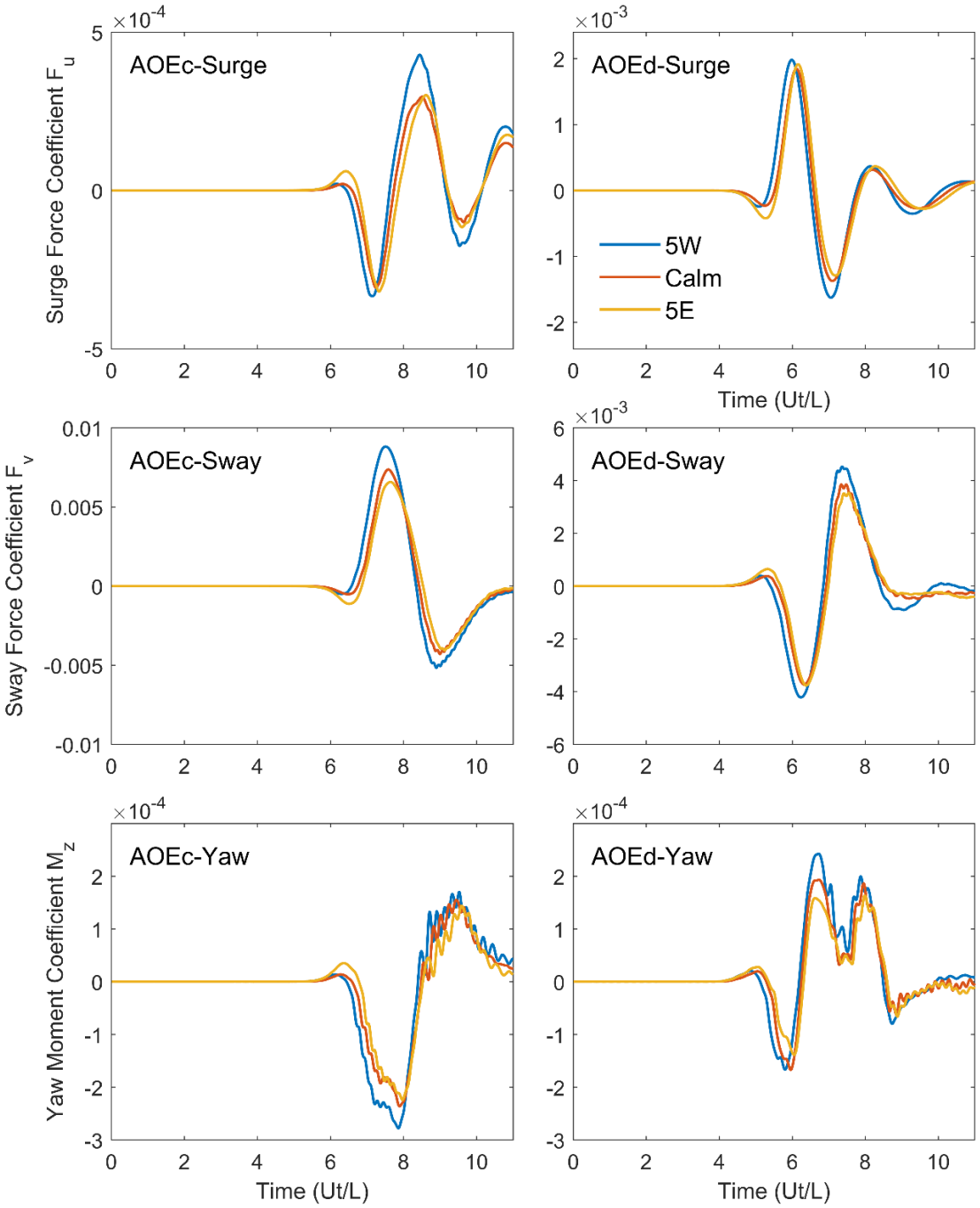

Fig. 26 Force and moment histories induced by an inbound ship at 7 kt with different drift angles

5.6. Two passing ships in head-on encounter at Craney Island

Passing ship simulations are conducted to examine the ship coupling effect with two passing ships in head-on encounter. The core parametric study in Group 1 of Table 3 includes 4 different inbound ship lanes and four different ship speeds. As the inbound ship moves away from the west bank, the minimum separation distance (sidewall to sidewall) between the two passing ships reduces from 216 ft to only 16 ft, resulting in a dramatic increase of the ship coupling effect.

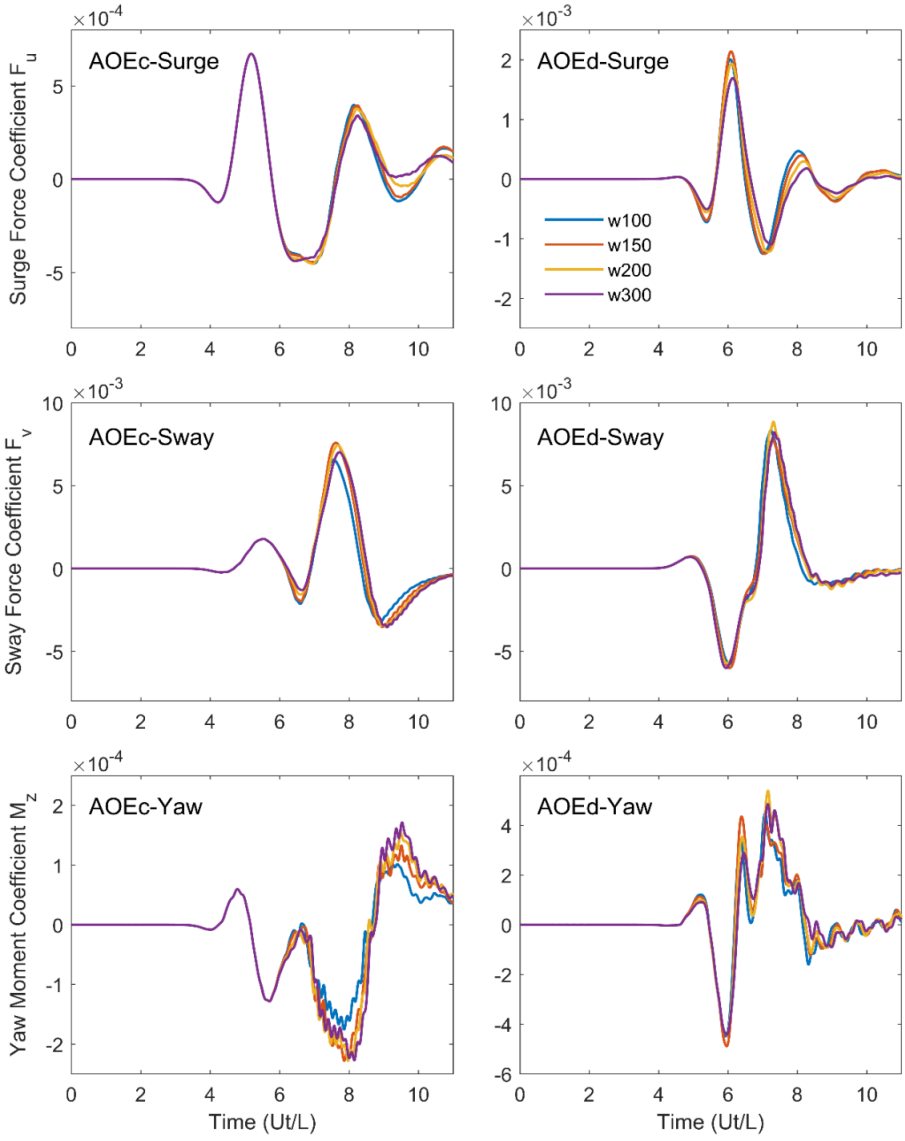

Fig. 27 Effect of ship lanes for two 7 kt head-on ships

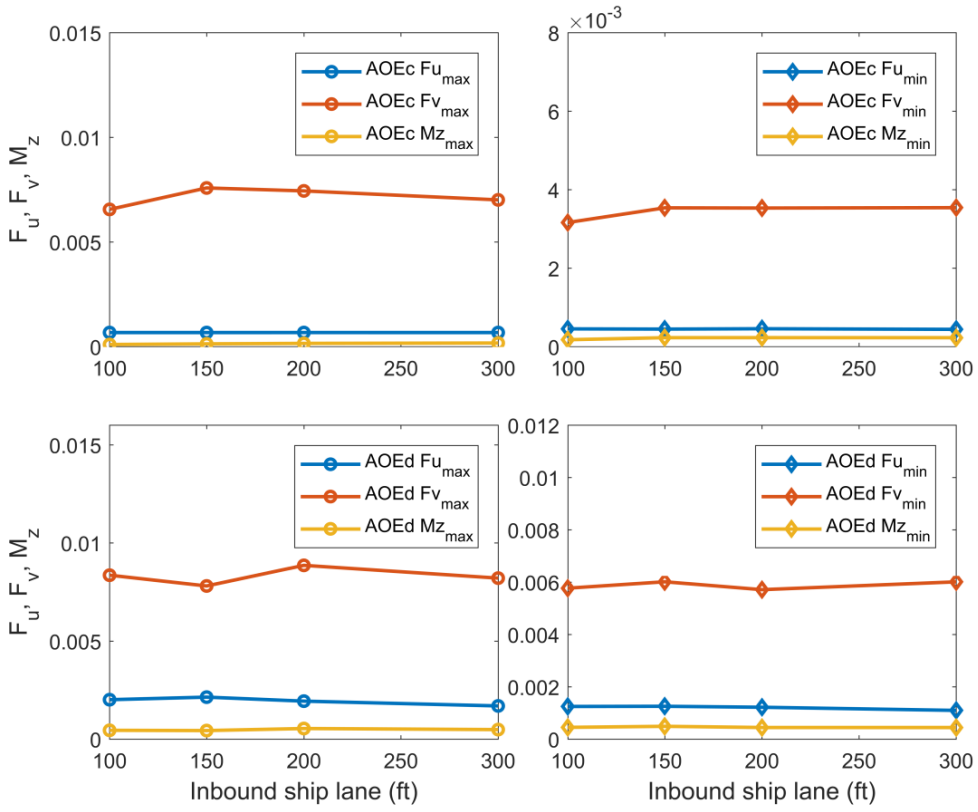

Fig. 28 Effect of ship lanes for two 7 kt head-on ships

Fig. 27 shows the forces and moment histories on the moored ships under different ship lane separation distances. Compared to the single passing ship cases, the effect of ship lanes are much more complex, not only from the combined influences of the outbound and inbound ships, but also due to the interactive coupling (i.e., sheltering effect) between the two ships. Fig. 28 illustrate the peak forces and moments as very flat curves and hardly any ship lane effect. The sheltering effect under head-on encounter is evidently even more pronounced at this site than at NAVSTA Norfolk, described in section 4.5.

6. Conclusions

In the present study, the Finite-Analytic Navier-Stokes (FANS) code has been employed in conjunction with the Compound Ocean Structure Motion Analysis (COSMA) program for time-domain simulation of the passing ship effects at both NAVSTA Norfolk and Craney Island Fuel Terminal sites. Detailed seabed bathymetry was constructed based on NOAA database for Virginia Beach, echo sounding data for dredged navigational channels and waterfront, and nautical charts for Norfolk harbor.

Coupled FANS/COSMA simulations were carried out for 57 cases at NAVSTA Norfolk and 55 cases at the Craney Island site. Core simulations were performed for the site-specific and vessel-specific conditions under the proposed dredged channel depth. In addition, pilot simulations were performed for stationary moored ships to identify the worst-case scenario at each site and to verify the effects of the mooring line and fender stiffness on motion responses of the moored ships. The simulation matrix covers several critical parameters including (1) lateral separation distance, (2) passing ship speed, (3) channel water depth, (4) passing ship coupling mode and encounter position, (5) drift angle, and (6) effect of single passing ship. All the key parameters on passing ship effects were addressed and detailed results presented.

It was found that the simulation results were affected by all the parameters studied. The ship lane studies at both simulation sites clearly showed the bank effect with the proposed channel depth, while the existing depth in Craney Island site produced hydrodynamic forces and moments decreasing monotonically away from the channel bank. The ship speed effect is straightforward, suggesting reducing passing ship speed as the most effective way to mitigate the impact of the passing ship effects on the ships moored at nearby piers. Head-on encounters at both sites show strong sheltering effect and very minor ship lane effect. Overtaking encounter is normally dominated by the fast ship, but the sheltering effect may be observed. The effect of the drift angle is also quite straightforward. When the bow of the passing ship turned toward the waterfront in cross winds, the increased suction pressure generated higher hydrodynamic forces and moments on the moored ships. When the ship bow turned away from the waterfront, its influences on the moored ships were very minor, with the force and moment magnitudes induced about the same as the calm wind condition.

It should be remarked that the scope of the present study is confined to a specific type of passing ships, specific types of moored ships and pier configurations, and symbolic fender and mooring line configurations. Possible future studies include more detailed and refined simulations to address (1) size and type of passing ships, (2) size and location of the moored ships, pier type, orientation, fender configuration, and mooring designs, (3) major dredging and channel improvement, (4) port security barriers, and other relevant assessment of passing ship effects.

Acknowledgements

This project is sponsored by US Navy NAVFAC MIDLANT Division. Mr. Steve Jones provided site information and operation guidelines. Colleagues at MIDLANT Division offered constructive leads on the simulation headings. Messrs. Robert O'Malley and James Georgo of Hydrographic Branch kindly provided echo sounding data at the waterfront and assisted in hydrographic data conversion. Texas A&M University High Performance Research Computing Center provided all required computing resources. All valuable supports are greatly appreciated.

References

Chen, H.C. and Huang, E.T. (2003a), "Numerical simulation of dynamic responses of a floating pier in ship berthing operations", Paper No. EM-2003-136, *16th ASCE Engineering Mechanics Conference*, University of Washington, Seattle, July 16-18.

Chen, H.C. and Huang, E.T. (2003b), "Time-domain simulation of floating pier and multiple-vessel interactions by a chimera RANS method", *Proceedings of the 7th International Symposium on Fluid Control, Measurement and Visualization*, Sorrento, Italy, August 25-28.

Chen, H.C. and Patel, V.C. (1988), "Near-wall turbulence models for complex flows including separation", *AIAA J.*, **26**(6), 641-648.

Chen, H.C., Chen, C.R. and Huang, E.T. (2018), "CFD simulation of site-specific passing ship effects on multiple moored ships", *Proceedings of the 28th International Ocean and Polar Engineering Conference*, Sapporo, Japan, June 10-15.

Chen, H.C., Lin, W.M, and Hwang, Y.W. (2002a), "Application of chimera RANS method for multiple-ship interactions in a navigation channel", *Proceedings of the 12th International Offshore and Polar Engineering Conference*, Kitakyushu, Japan, May 26-31.

Chen, H.C., Lin, W.M. and Hwang, Y.W. (2002b), "Turbulent flow induced by multiple-ship operations in confined water", Paper No. EM-2002-123, *15th ASCE Engineering Mechanics Conference*, Columbia University, New York, June 2-5.

Chen, H.C., Lin, W.M. and Hwang, Y.W. (2002c), "Validation and application of chimera RANS method for ship-ship interactions in shallow water and restricted waterway", *Proceedings of the 24th Symposium on Naval Hydrodynamics*, Fukuoka, Japan, July 8-13.

Chen, H.C., Lin, W.M., Liut, D.A. and Hwang, W.Y. (2003), "An advanced viscous flow computational method for ship-ship interactions in shallow and restricted waterway", MARSIM'03, Japan.

Huang, E.T. and Chen, H.C. (2003), "Ship berthing at a floating pier", *Proceedings of the 13th International Offshore and Polar Engineering Conference*, Honolulu, Hawaii, May 25-30.

Huang, E.T. and Chen, H.C. (2006), "Passing ship effects on moored vessels at piers", *Proceedings of the Prevention First 2006 Symposium, An Onshore and Offshore Pollution Prevention Symposium and Technology Exhibition*, Long Beach, California.

Huang, E.T. and Chen, H.C. (2007), "Influence of site specifics on passing ship effects", *Proceedings of the 17th International Offshore and Polar Engineering Conference*, July 1-6, Lisbon, Portugal.

Huang, E.T. and Chen, H.C. (2010), "Passing ship effects at typical waterfronts", *Proceedings of the ASCE PORTS 2010 Conference*, Jacksonville, Florida, April 25-28.

Huang, E.T., Chen, H.C. and Chen, C.R. (2018), "Engineering concerns of passing ship effect at typical waterfronts", *Proceedings of the 28th International Ocean and Polar Engineering Conference*, Sapporo, Japan, June 10-15.

Huang, T.S. (1990), "Interaction of ships with berth at floating terminals", TM-65-90-03, Naval Civil Engineering Laboratory, Port Hueneme, California.

Pontaza J.P., Chen H.C. and Reddy J.N. (2005), "A local-analytic-based discretization procedure for the numerical solution of incompressible flows", *Int. J. Numer. Meth. Fl.*, **49**(6), 657-699.

Taylor L.A., Eakins, B.W., Carignan, K.S., Warnken, R.R., Sazonova, T., Schoolcraft, D.C. and Sharman, G.F. (2008), "Digital elevation model of Virginia Beach, Virginia: Procedures, data sources and analysis", NOAA Technical Memorandum NESDIS NGDC-7, National Geophysical Data Center, Boulder, Colorado.

MK